RI.
SE

DIVISION SAFETY AND TRANSPORT
FIRE PROTECTION

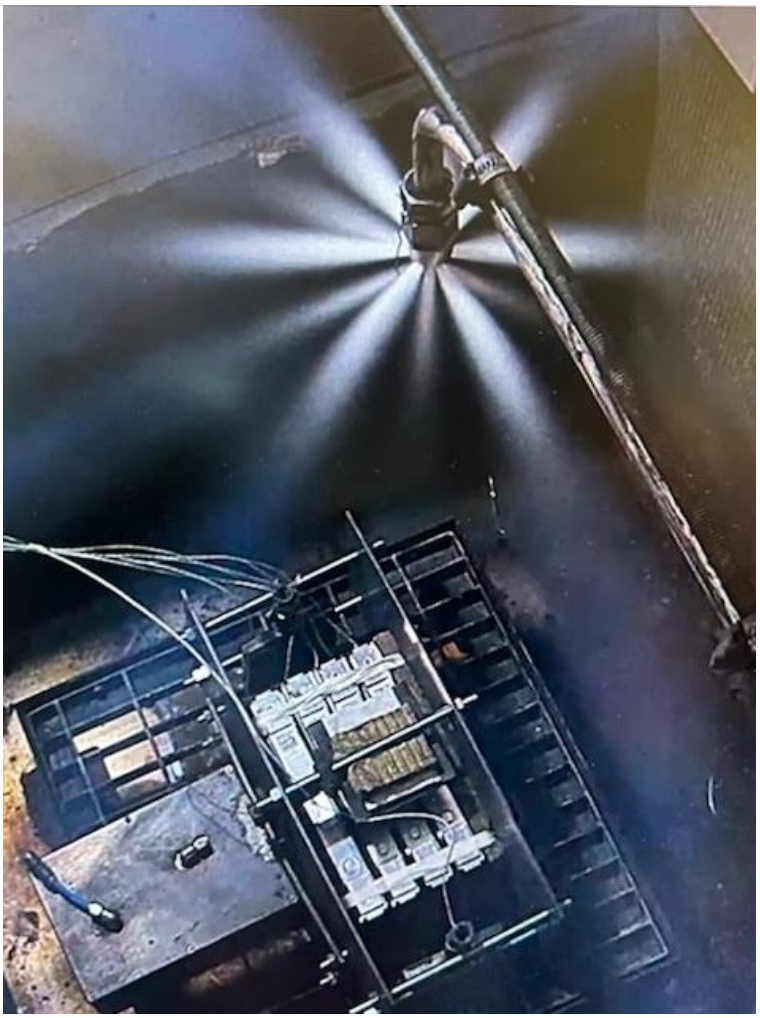

Small-scale fire suppression tests of lithium-ion battery cells using carbon dioxide

Magnus Arvidson
Anna Karlsson
Örjan Westlund

RISE Report 2026:102

Small-scale fire suppression tests of lithium-ion battery cells using carbon dioxide

Magnus Arvidson
Anna Karlsson
Örjan Westlund

© RISE Research Institutes of Sweden

Abstract

Small-scale fire suppression tests of lithium-ion battery cells using carbon dioxide

This report presents a series of small-scale tests conducted within the Carbon diOxide Fire Fighting Experimental Evaluation (COFFEE) project to investigate the influence of carbon dioxide on lithium-ion battery fires and thermal runaway propagation. The work comprised preliminary cold discharge tests followed by two test series involving lithium-ion battery cells exposed to free-burn and fire-suppression conditions.

The cold discharge tests were used to develop the test methodology and establish a carbon dioxide concentration of approximately 45 % within a customised test compartment. Four battery cell types were investigated, including prismatic nickel-manganese-cobalt oxide (NMC) cells, prismatic lithium iron phosphate (LFP) cells, and cylindrical NMC cells. Thermal runaway was initiated either by external heating or by nail penetration. Note: Despite repeated attempts, the LFP cells could not be successfully ignited and were therefore excluded from the tests. Free-burn tests were conducted to provide benchmark data, while suppression tests evaluated different carbon dioxide concentrations, corresponding to oxygen levels of approximately 11.5 % and 6.3 %.

The results showed that carbon dioxide reduced fire severity when thermal runaway was initiated by external heating, particularly for the cylindrical cells. Peak temperatures were substantially reduced as oxygen concentrations decreased, indicating a suppression of flaming combustion and external heat transfer. For larger prismatic (NMC) cells, the reduction in fire severity was more limited, and no significant delay in thermal propagation was observed. When thermal runaway was initiated by nail penetration, carbon dioxide had little measurable effect on peak temperatures or propagation rates, suggesting that the process was dominated by internal exothermic reactions largely independent of the surrounding atmosphere. Overall, the effectiveness of carbon dioxide was found to depend strongly on battery design, propagation mechanisms, and the method used to initiate thermal runaway.

Key words: Fire suppression, carbon dioxide, lithium-ion batteries, small-scale fire tests

RISE Research Institutes of Sweden AB

RISE Report 2026:102
ISBN: 978-91-90193-35-8

Borås 2026

© RISE Research Institutes of Sweden

Content

Abstract **1**
Content **2**
Preface **3**
Summary **4**
1 Cold discharge tests **6**
1.1 Objective 6
1.2 The test compartment 6
1.3 The carbon dioxide nozzle 8
1.4 Measurements and instrumentation 9
1.5 Test objective 10
1.6 Test program 10
1.7 Test results 10
1.8 General observations 11
2 Free-burn and fire suppression tests **13**
2.1 Objective 13
2.2 The battery cells used in the tests 13
2.3 Preparation, measurements and instrumentation 14
2.4 First series of tests 19
2.4.1 General 19
2.4.2 The heating element 19
2.4.3 Fire test procedures 20
2.4.4 Results 20
2.5 Second series of tests 30
2.5.1 General 30
2.5.2 The nail penetration equipment 30
2.5.3 Fire test procedures 30
2.5.4 Results 31
3 Discussion **41**
4 Conclusion **43**

© RISE Research Institutes of Sweden

Preface

The small-scale fire suppression tests documented in this report were conducted as part of the Carbon diOxide Fire Fighting Experimental Evaluation (COFFEE) project. The overall objective of the project is to improve the safety of transporting lithium-ion battery-powered vehicles in the ro-ro spaces on board maritime vehicle carriers. Specifically, the project investigates the effectiveness of conventional low-pressure carbon dioxide fire-extinguishing systems for controlling and suppressing fires involving battery electric vehicles.

The project begun with a comprehensive literature study to describe the fire suppression mechanisms, personnel safety issues and installation guidelines for carbon dioxide systems. Additionally, it collected existing data on fire incidents on ro-ro vehicle carriers, the performance of the fixed carbon dioxide system (if used) and lithium-ion battery fire suppression tests using carbon dioxide. This part is documented in RISE Report 2024:75 [1]. Computer modelling as well as large scale-fire suppression tests were also part of the project. The project is summarized in RISE Report 2026:101.

The project is led and coordinated by RISE Research Institutes of Sweden. The project's reference group comprises experts from a range of organizations within the field. The active engagement of the participants and the valuable discussions throughout the project are gratefully acknowledged. The authors would also like to acknowledge the battery cell suppliers for providing the cells used in the tests and for their valuable support throughout the project.

The project was funded by Stiftelsen Sveriges Sjömanshus (the Swedish Mercantile Marine Foundation) and Trafikverket (the Swedish Transport Administration).

Cover photo: Örjan Westlund, RISE Research Institutes of Sweden. All other photographs in this report were taken by staff members of RISE Research Institutes of Sweden.

1 Arvidson, Magnus and Karlsson, Anna, "Literature study: The performance of carbon dioxide systems on ro-ro vehicle carriers", RISE Report 2024:75, ISBN: 978-91-89971-36-3, Göteborg 2024

© RISE Research Institutes of Sweden

Summary

This report documents a series of small-scale experiments performed within the COFFEE project to evaluate the influence of carbon dioxide on fires involving lithium-ion battery cells. The project aims to improve the understanding of how conventional fixed carbon dioxide systems may perform in battery electric vehicle fire scenarios relevant to marine vehicle carriers. The work consisted of cold discharge tests to establish the experimental methodology, followed by free-burn and fire suppression tests involving different lithium-ion battery cell types.

The cold discharge tests were carried out in a 3.4 m³ compartment containing an open-top steel enclosure designed to retain the carbon dioxide atmosphere around the test specimens. The results demonstrated that approximately 4.5 kg of carbon dioxide produced an atmosphere containing about 45 % carbon dioxide, corresponding to approximately 11.5 % oxygen. The tests also showed that the enclosure successfully maintained the reduced-oxygen environment for extended periods.

Two series of fire suppression tests were subsequently performed. In the first series, thermal runaway was initiated using an external heating element. Tests were conducted on large prismatic NMC cells (denoted V-cells) and cylindrical NMC cells (denoted C-cells). LFP cells were initially included in the test programme; however, as they could not be successfully ignited, they were excluded from the fire suppression tests. Free-burn tests served as benchmarks for the subsequent fire suppression tests, providing reference data on the oxygen concentration within the test compartment, the surface temperatures of the battery cells, and the surface temperatures measured by the surrounding Plate Thermometers. For the prismatic V-cells, the presence of carbon dioxide reduced peak temperatures of the Plate Thermometers slightly, but the influence on thermal runaway propagation was limited. The time required for fire development remained largely unchanged. In contrast, cylindrical C-cells showed a more pronounced response. Peak temperatures of the Plate Thermometers decreased from approximately 265 °C in free-burn conditions to 175 °C and 124 °C at reduced oxygen concentrations caused by the carbon dioxide discharge, indicating a substantial reduction in fire severity. These findings suggest that carbon dioxide can be particularly effective when thermal propagation depends on flaming combustion and external heat transfer between cells.

The second series of tests investigated thermal runaway initiated by nail penetration, representing internal cell damage. Prismatic NMC cells (denoted N-cells and V-cells) and LFP cells were tested. Thermal runaway of the LFP cells could not be achieved despite repeated attempts, illustrating their greater thermal stability. For both N-cell and V-cell configurations, carbon dioxide had little measurable effect on fire severity. Peak temperatures in the suppression tests were similar to, or even higher than, those recorded in the corresponding free-burn tests. Likewise, reduced oxygen concentrations did not consistently increase the time required for thermal propagation. These results indicate that once thermal runaway is initiated by direct internal damage, the process is largely driven by exothermic reactions inside the cells, which are not significantly affected by the surrounding atmosphere.

© RISE Research Institutes of Sweden

A key challenge throughout the study was controlling the oxygen concentration during the tests. The fires themselves altered the compartment atmosphere through oxygen consumption, generation of combustion gases, and pressure-driven venting of the carbon dioxide through the pressure-relief hatch. Consequently, the oxygen concentration during thermal runaway often differed from the intended value established before ignition. This effect was particularly evident in the nail-penetration tests, where oxygen concentrations frequently increased after thermal runaway due to displacement of the pre-established carbon dioxide atmosphere.

Overall, the study shows that carbon dioxide can reduce the severity of lithium-ion battery fires, but its effectiveness depends strongly on battery design, propagation mechanisms, and the initiation method. The largest benefit was observed for smaller cylindrical cells, where suppression of flames and external heat transfer appeared to limit fire development. In contrast, the influence of carbon dioxide on thermal runaway propagation in large prismatic cells was limited, especially when thermal runaway was initiated by nail penetration. The findings suggest that carbon dioxide is most effective when flaming combustion contributes significantly to propagation and less effective when propagation is dominated by internal heat transfer and exothermic decomposition reactions. Further studies with improved atmospheric control and larger test matrices are recommended to better quantify these effects.

© RISE Research Institutes of Sweden

1 Cold discharge tests

1.1 Objective

This part of the report documents cold discharge carbon dioxide tests conducted in June 2024 at RISE, Borås, Sweden. The tests were conducted to establish a test set-up and test procedure for upcoming small-scale fire suppression tests using lithium-ion battery cells.

1.2 The test compartment

The internal size of the test compartment was 1250 mm by 1250 mm by 2200 mm (H), corresponding to an internal volume of 3.4 m^3. The compartment was constructed from nominally 10 mm thick non-combustible cement fibre boards with an outer layer of nominally 15 mm thick plywood boards. The entire front wall of the compartment was removable to provide easy access to the compartment. Figure 1 shows the test compartment.

The ceiling was fitted with a 500 mm by 500 mm opening having a hatch with hinges, which acted as a pressure-relief vent of the over-pressure generated by the outflow of carbon dioxide. During the series of tests, the function of the hatch was improved and a weight load consisting of a 5 L water bottle was positioned on the top of the hatch to increase its weight.

An open-top box, internally sized 1000 mm by 1000 mm by 800 mm (H) was positioned at the floor of the test compartment. The box was made from steel sheets, nominally 1 mm thick which were seam-welded. The intent of the box was to provide an air-tight volume, collecting the carbon dioxide gas, to result in a pro-longed hold time around the upcoming test objects. The bottom of the steel-sheet box had an outlet, where a 1" pipe and a ball valve were connected, allowing the dispense of gas after each test. Figure 2 shows the arrangement.

© RISE Research Institutes of Sweden

Figure 1 The test compartment.

© RISE Research Institutes of Sweden

Figure 2 The position of the carbon dioxide cylinder (on a load cell) and the outlet from the test compartment.

The test set-up was positioned inside the small fire test hall at RISE.

1.3 The carbon dioxide nozzle

A pendent, multi-orifice nozzle was positioned in the test compartment at a vertical distance of 1300 mm above the floor. The inlet of the nozzle had a removable washer, allowing the inlet orifice diameter to be varied from 3 mm to 10 mm in increments of 0.5 mm. By varying the inlet orifice diameter, different discharge times can be selected, given a specific amount of carbon dioxide. The pendent position is shown in Figure 3.

The nozzle (Firesafe 6-01-3465-1201-Nozzle Body 1/2" BSP) was made by Ginge-Kerr and was purchased from Firesafe Sverige AB.

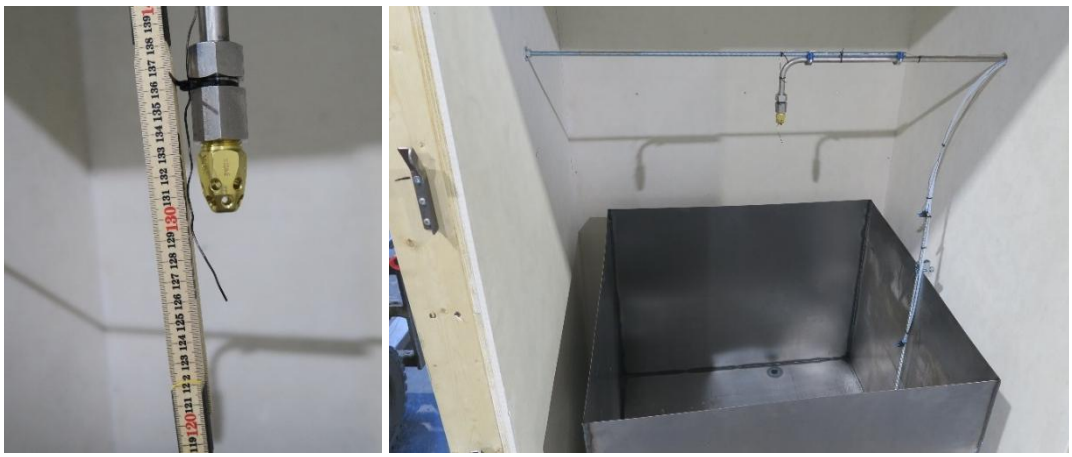

Figure 3 The pendent, multi orifice nozzle and its position in the test compartment.

The nozzle was positioned 500 mm above the top edge of the steel box and was connected to the carbon dioxide pressure cylinder with a 1100 mm stainless pipe (internal diameter 11 mm) and a 1000 mm flexible hose (1/2").

© RISE Research Institutes of Sweden

The carbon dioxide pressure cylinder had a nominal volume of 13.4 L and was filled with 0.75 kg/L by the supplier (Air Liquide), i.e., it contained a nominal weight of 10 kg of carbon dioxide. The nominal filling pressure was 50.5 bar.

1.4 Measurements and instrumentation

The following measurements were made, refer to Table 1:

Table 1 The measurements and the associated measurement channels.

Channel	Measurement	Position
C1	Temperature	At the oxygen sampling point of C4 (500 mm)
C2	Temperature	At the oxygen sampling point of C5 (1000 mm)
C3	Temperature	50 mm below the discharge nozzle
C4	Oxygen concentration	500 mm above floor (inside the steel-sheet box)
C5	Oxygen concentration	1000 mm above floor (at the top edge of the stee-sheet box)
C6	Weight and weight loss	Load cell

Sheathed Ø=0.5 mm, Type K thermocouple wiring was used for the temperature measurements.

The load cell had a maximum capacity of 60 kg (Combics 3, KWP02402).

The oxygen concentrations were measured with two Xtreme instruments (inventory numbers 900864 and 900866), refer to Figure 4.

Figure 4 The oxygen concentration measurement instruments.

© RISE Research Institutes of Sweden

1.5 Test objective

The objective of the tests was to find a combination of 1) an amount of carbon dioxide and 2) a nozzle inlet orifice diameter that provided:

- A carbon dioxide concentration of around 45 % (at measurement point C4).
- An outflow (discharge) time of around 60 seconds.

1.6 Test program

The following tests were conducted on June 26 (Tests 1 – 5) and on June 27, 2024 (Tests 6 – 8), refer to Table 2.

Table 2 The test program.

Test	Nominal amount CO_2 [kg]	Orifice diameter [mm]	Notes
1	5	3.0	No weight loss measurements available.
2	5	5.0	-
3	4.5	5.0	Only 3 kg discharged according to the measurements. The test was repeated in Test 4. Probably too much gas was tapped off prior the test.
4	4.5	5.0	Repeat of Test 3. This data seems correct.
5	5.5	5.0	-
6	6.0	5.0	-
7	8.0	5.0	-
8	10.0	5.0	The full amount of gas in the pressure cylinder was used.

1.7 Test results

Table 3 below summarises the main test parameters and results.

Table 3 The main test parameters and results.

Test	Nominal amount CO_2 [kg]	Measured amount CO_2 [kg]	Orifice diameter [mm]	Min. O_2 concentration [%] 500 mm above floor	Calculated CO_2 concentration [%] 500 mm above floor	Min. temp. [°C] 500 mm above floor	Discharge time [s*/s**]
1	5.0	N/A	3.0	10.94	47.90	-11	N/A
2	5.0	5.09	5.0	10.58	49.62	-27	13/50
3	4.5	2.99	5.0	13.50	35.71	+1	6/25
4	4.5	4.72	5.0	10.93	47.95	-15	11/50
5	5.5	4.30	5.0	11.40	45.71	-16	11/50
6	6.0	6.52	5.0	8.83	57.95	-32	16/40
7	8.0	7.89	5.0	7.68	63.43	-37	18/44
8	10.0	9.90	5.0	6.20	70.48	-52	24/50

*) Until the outflow of the gas phase started, as determined by derivation of the weight loss data.
**) Until the outflow of the gas phase ceased, as determined from the weight loss data.

© RISE Research Institutes of Sweden

Based on the test results, it was determined that 4.3 kg of carbon dioxide provided the target concentration of 45 % and a discharge time of 50 seconds when a 5.0 mm inlet orifice diameter was used. As evaluating the effects of higher carbon dioxide concentrations may be relevant for the upcoming fire suppression testing, additional tests were conducted with larger gas volumes. In the final test, the pressure cylinder was discharged completely.

1.8 General observations

The oxygen concentration measured 500 mm above floor (inside the steel-sheet box) remained basically constant during the entire 60-minute hold time. This proved that the concept of an air-tight, open-top box worked well.

The oxygen concentration at the measurement point 1000 mm above floor was not equally constant, indicating leakage from the actual compartment. The airtightness of the test compartment was slightly improved after Test 1, by sealing some gaps, and the improved tightness was clearly visible in the test data. In later tests (Tests 6 and 7) some leakage was observed again.

Figure 5 shows the calculated concentration of carbon dioxide as a function of the amount of gas. The graph shows the linear relationship based on seven tests. The test with the least amount of gas (Test 3) is excluded in the latter graph, as it generated a concentration less than the 45 % threshold.

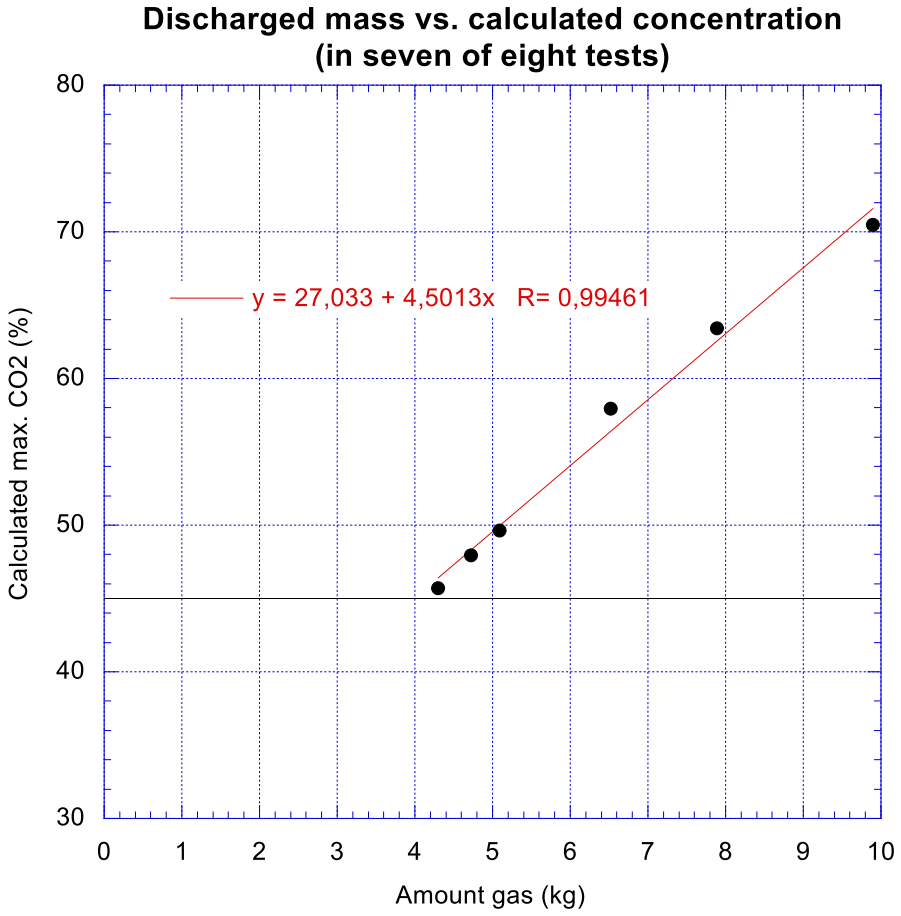

Figure 5 The calculated concentration of carbon dioxide as a function of the amount of gas.

© RISE Research Institutes of Sweden

Figure 6 shows the measured oxygen concentrations for all tests in two graphs, demonstrating the extent to which the oxygen concentration remained constant during the 60-minute hold period.

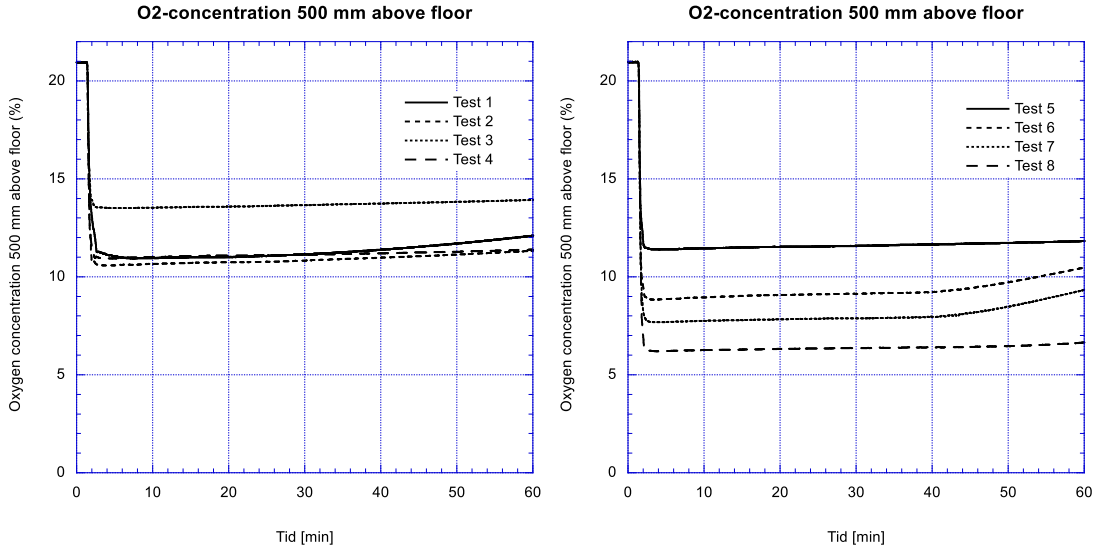

Figure 6 The measured oxygen concentration for all tests.

© RISE Research Institutes of Sweden

2 Free-burn and fire suppression tests

2.1 Objective

The test compartment described in Section 1.2 was used for all tests presented in this section. The tests were conducted during two separate test series, in October 2025 and in February 2026. In the first test series, thermal runaway of battery cells was initiated using a heating element, whereas in the second series, it was initiated by nail penetration.

During both test series, free-burn fire tests were conducted. These tests served as benchmarks for the subsequent fire suppression tests, providing reference data on the oxygen concentration within the test compartment, the surface temperatures of the battery cells, and the surface temperatures measured by the surrounding Plate Thermometers.

2.2 The battery cells used in the tests

Four types of battery cells were used in the tests, refer to Table 4.

Table 4 The type of cells used in the tests.

Designation	N-cells	V-cells	EVE-cells	C-cells
Type	Prismatic automotive li-ion cells	Prismatic automotive li-ion cells	Prismatic li-ion cells	Cylindrical automotive li-ion cells
Cell chemistry	NMC	NMC	LFP	NMC
Nominal geometrical size	L: 236 mm W: 115 mm T: 32 mm	L: 220 mm W: 102 mm T: 33 mm	L: 174 mm W: 207 mm T: 72 mm	L: 70 mm Dia: 21 mm
Nominal voltage (min – max)	3.7 V (2.8 V ~ 4.2 V)	3.7 V (1.8 V ~ 4.25 V)	3.2 V (2.0 V ~ 3.65 V)	4.2 V
Energy capacity	157 Ah	120 Ah	280 Ah	4.8 Ah
Energy capacity	574 Wh	442 Wh	896 Wh	17.5 Wh
Total capacity	2 296 Wh	1 768 Wh	3 584 Wh	105 Wh
Nominal weight	2.2 kg	1.8 kg	5.5 kg	70 g
Total weight	8.8 kg	7.2 kg	22 kg	420 g

Nickel-manganese-cobalt oxide (NMC) cells use lithium, nickel, manganese, and cobalt in the cathode material, typically combined with a graphite or graphite-silicon anode. Key characteristics of NMC chemistry include high energy density, making it well suited

© RISE Research Institutes of Sweden

for applications requiring a long driving range, and moderate thermal stability, with a higher risk of oxygen release and thermal runaway compared to LFP cells [2, 3].

Lithium iron phosphate (LFP) cells use $LiFePO_4$ as the cathode material and typically graphite as the anode. Key characteristics of LFP chemistry include high thermal stability and low risk of oxygen release, lower energy density compared to NMC chemistry, but better tolerance to high temperatures and mechanical abuse [3].

All cells were charged to full capacity before being used in the tests.

2.3 Preparation, measurements and instrumentation

The test compartment was positioned beneath the small-scale ("furniture") calorimeter located in the large fire test hall at RISE. The calorimeter is equipped with a collection hood measuring 3 m by 3 m, which is connected to an exhaust ventilation duct designed to capture and extract all combustion products generated during the tests. By collecting the complete combustion gas stream, the system enabled continuous measurement of the heat release rate (HRR) using the oxygen consumption calorimetry principle. It should be noted, however, that heat release rate measurements were only possible during tests conducted with the ceiling of the test compartment removed, primarily the free-burn tests. Gas temperature, velocity, the generation of gaseous species such as CO_2 and CO, and the depletion of O_2 were measured in the exhaust duct. All measurement equipment in the exhaust duct and the calculation model for the heat release rate were based on the requirements in ISO 9705-1:2017 [4]. The ventilation flow rate of the equipment was 8000 m^3/h in all tests.

Four prismatic cells were placed in direct contact with each other and positioned between two 20 mm thick sheets of rock wool insulation. The row of cells was then clamped between two 3 mm thick steel plates, which were held together by five 10 mm thick threaded clamps. Figure 7 shows the arrangement.

2 Jin, Guangyao; Zhao, Wanwei; Zhang, Jianing; Liang, Wenyu; Chen, Mingyang; and Xu, Rui., "High-Temperature Stability of $LiFePO_4$/Carbon Lithium-Ion Batteries: Challenges and Strategies", Sustainable Chemistry, 6(1), 7, 2025, https://doi.org/10.3390/suschem6010007

3 "Safety Evaluation of Lithium-Ion Battery Cathode and Anode Materials Using Differential Scanning Calorimetry", Available at: https://www.tainstruments.com/applications-notes/safety-evaluation-of-lithium-ion-battery-cathode-and-anode-materials-using-differential-scanning-calorimetry/ (Accessed 2026-09-01)

4 ISO 9705-1:2017, "Reaction to fire tests - Room corner test for wall and ceiling lining products - part 1: Test method for a small room configuration (ISO 9705-1:2016, IDT)", Approved: 2017-02-15

© RISE Research Institutes of Sweden

Figure 7 The arrangement of the prismatic cells, with photos showing outer steel plates, the rock wool insulation and the position of the heating element.

These clamps also served as mounting points for three Plate Thermometers. Each Plate Thermometer consists of a 0.7 mm thick Inconel 600 plate with a front surface measuring 100 mm by 100 mm. A sheathed thermocouple is spot-welded to the plate, which is insulated on the back side. The device is sensitive to convective heat transfer, but in comparison with a conventional thermocouple it is significantly more responsive to thermal radiation [5, 6]. The devices were purchased from Pentronic AB.

One Plate Thermometer was mounted vertically 50 mm above the top of the package of the prismatic cells (C26). Another Plate Thermometer was positioned horizontally, 50 mm from the short sides of the cells, respectively (C27-C28). Figure 8 shows the arrangement. For test evaluation, the average of the peak surface temperatures measured by the three Plate Thermometers was calculated.

5 Wickström, Ulf, ”The plate thermometer - A simple instrument for reaching harmonized fire resistance tests”, SP Report 1989:03, Swedish National Testing and Research Institute, Borås, 1989

6 Wickström, Ulf, ”The plate thermometer - A simple instrument for reaching harmonized fire resistance tests”, Fire Technology, Volume 30, No. 2, 1994

© RISE Research Institutes of Sweden

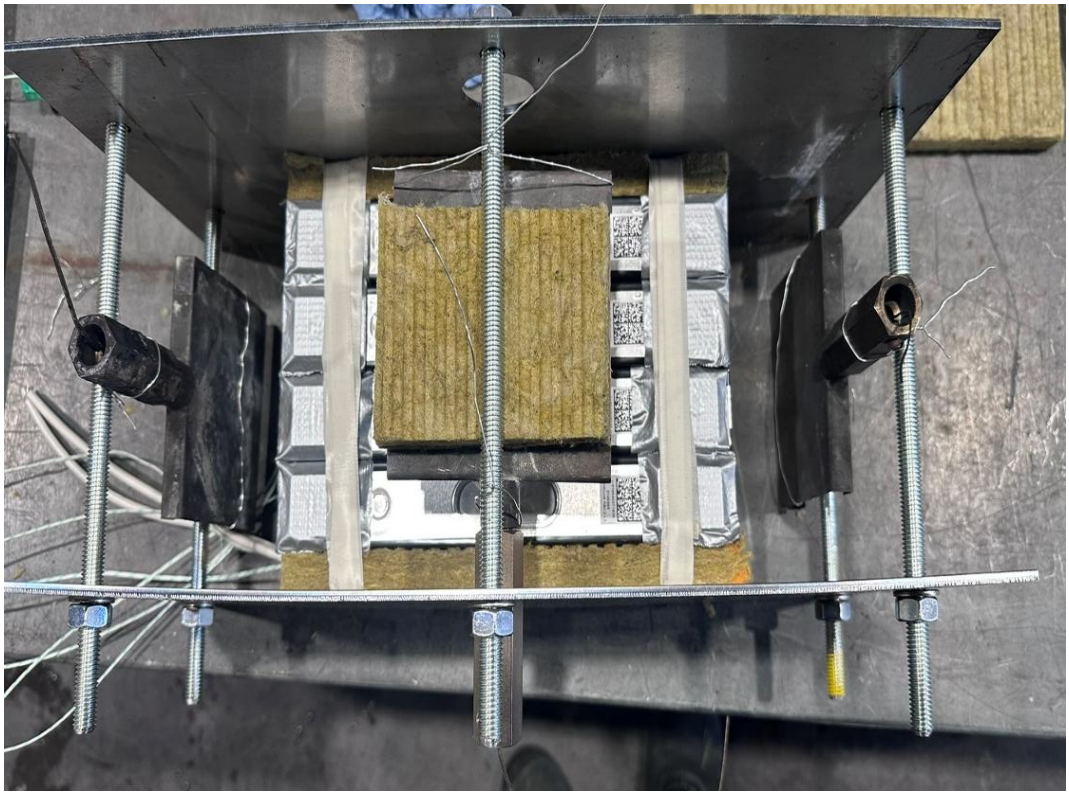

Figure 8 The positions of the Plate Thermometers: One was mounted vertically 50 mm above the top of the package of prismatic cells (C26). Another Plate Thermometer was positioned horizontally, 50 mm from the short sides of the cells, respectively (C27-C28).

The surface temperature of the prismatic N- and EVE-cells was measured using thermocouples positioned at the centre of the outermost face adjacent to the rock wool insulation (C21), at the centre between each cell (C22-C24), and at the centre of the opposite outer face, also facing the rock wool insulation (C25). The prismatic V-cells were electrically interconnected in pairs, which prevented thermocouples from being placed between cells 1 and 2 and between cells 3 and 4. Consequently, temperature measurements for the V-cells were limited to the outer faces of the cell stack (C21 and C25) and the central position between cells 2 and 3 (C23).

The gas temperatures in front of the carbon dioxide discharge nozzle (C30) and at the position of the oxygen measurement sampling point (C31), were measured.

The oxygen concentration inside the test compartment was measured at level with the battery cells. For redundant reasons, two Xtreme oxygen concentrations measurement instruments (inventory numbers 900864 and 900866) were used.

Finally, the weight and weight loss of the carbon dioxide cylinder was measured (C34).

Table 5 shows the measurements and the associated measurement channels.

© RISE Research Institutes of Sweden

Table 5 The measurements and the associated measurement channels.

Channel	Measurement	Position
C21	Surface temperature	The surface with the thermal element (facing the rock wool insulation)
C22	Surface temperature	Between cells 1 and cell 2. Note: Not relevant for the V-cells.
C23	Surface temperature	Between cell 2 and cell 3.
C24	Surface temperature	Between cell 3 and cell 4. Note: Not relevant for the V-cells
C25	Surface temperature	Between cell 4 and the rock wool insulation.
C26	Plate Thermometer	Plate Thermometer above the top of the package of cells
C27	Plate Thermometer	Plate Thermometer to the left of the package of cells.
C28	Plate Thermometer	Plate Thermometer to the right of the package of cells.
C30	Gas temperature	In front of the carbon dioxide discharge nozzle.
C31	Gas temperature	At the position of the oxygen measurement sampling point
C32	Oxygen conc.	At level with the battery cells
C33	Oxygen conc.	Same position as above (for redundancy)
C34	Weight and weight loss of the gas cylinder	Load cell (60 kg load cell)

Sheathed Ø=0.5 mm, Type K thermocouple wiring was used for the temperature measurements.

The cylindrical C-cells were arranged in a 2 by 8 array, refer to Figure 9. The heating element was placed facing one of the short sides of the array, with a thin layer of ceramic fibre insulation positioned behind it. The array of cells was held together by a cage made from a perforated steel plate, secured by metal wire. It should be noted that the overall size and weight of the package of cylindrical cells was significantly less compared to the packages with the prismatic cells.

The measurements and the instrumentation were like those of the prismatic cells.

The package containing the cells, regardless of cell type, was placed on a small table with a steel grating top and subsequently positioned inside the open-top steel-sheet box located within the test compartment, refer to Figure 10. This arrangement ensured that the package was securely supported while allowing carbon dioxide gas to access it from both above and below. The internal walls of the steel-sheet box were lined with 20 mm thick rock wool insulation panels.

© RISE Research Institutes of Sweden

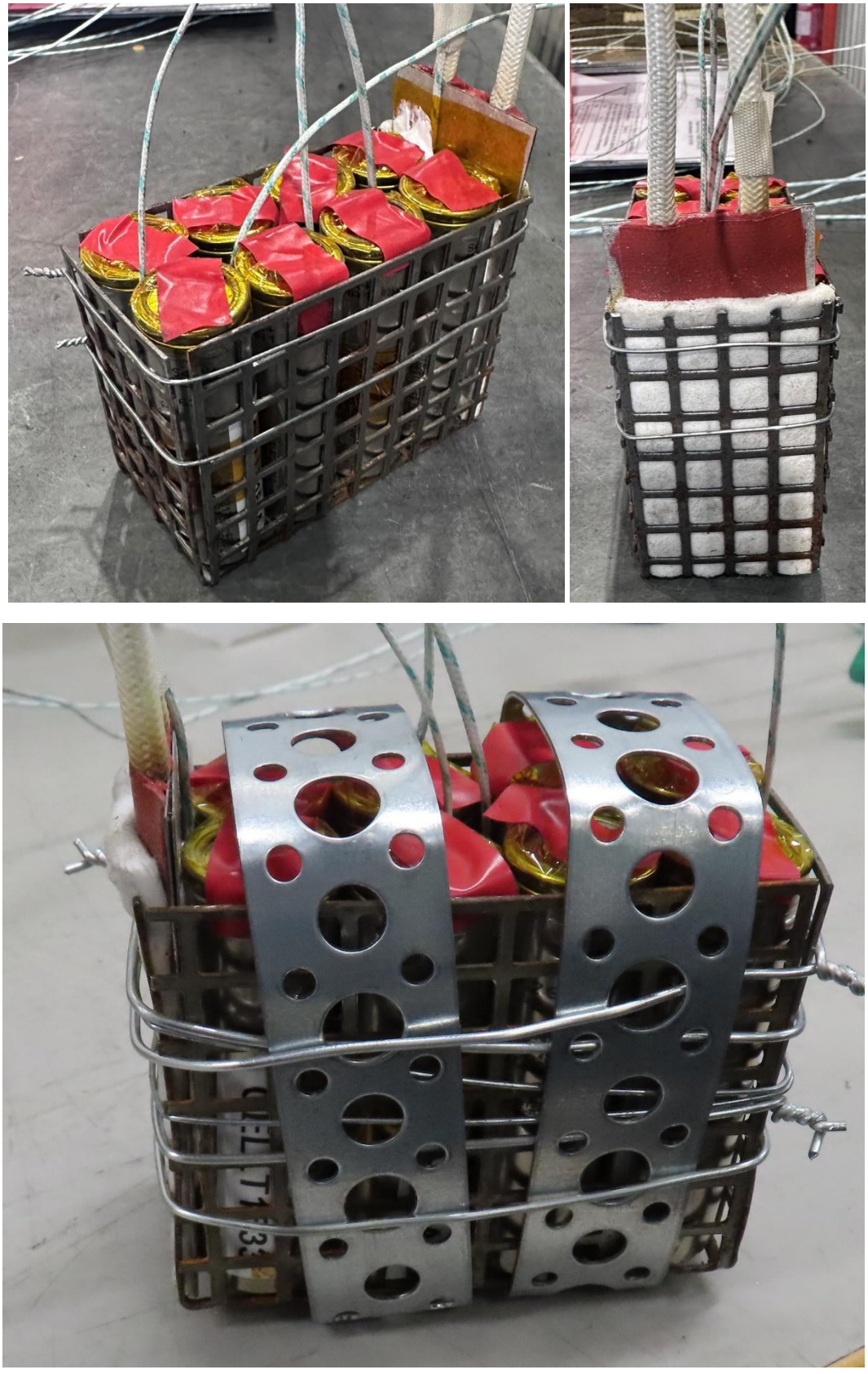

Figure 9 The arrangement of the cylindrical cells, with the position of the heating element. The bottommost photo shows the reinforced cage.

© RISE Research Institutes of Sweden

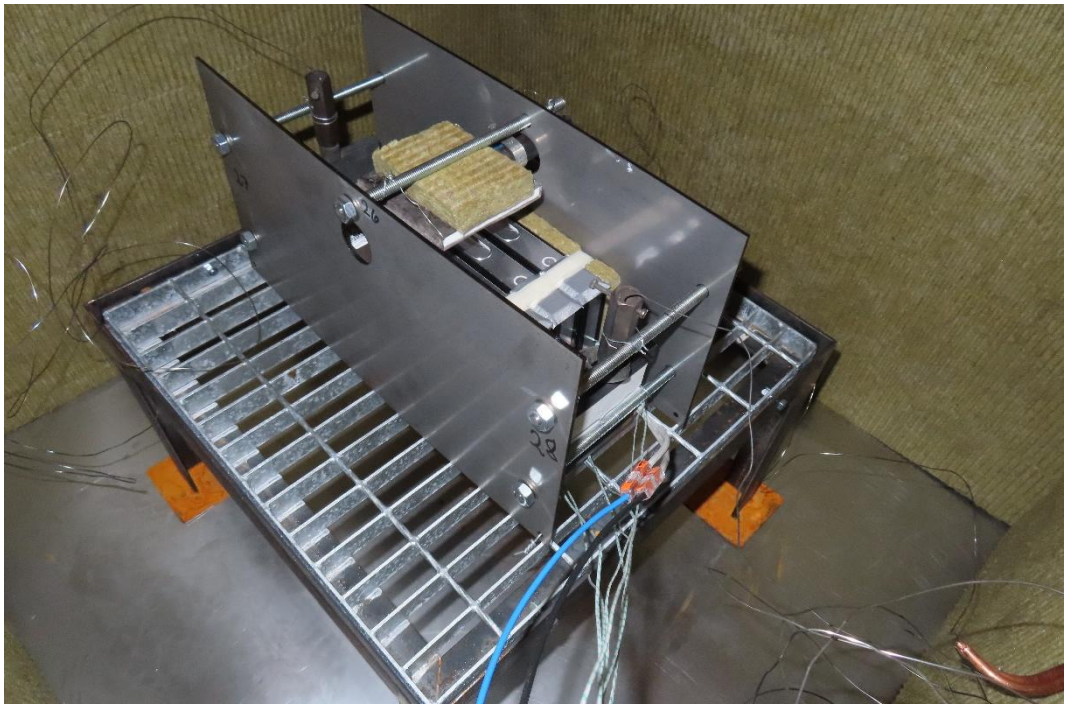

Figure 10 The small table with a steel grating top that was positioned inside the open-top steel-sheet box located within the test compartment. At the right-hand side corner of the photo, the sampling lines (copper pipes) for the oxygen concentration measurements can be observed.

2.4 First series of tests

2.4.1 General

During these tests, ignition was initiated using a heating element positioned either at the side of one of the outermost prismatic cells (between the cell and the insulation board) or at the short side of the array of cylindrical cells.

The EVE-cells were not included in the tests. Parallel testing at RISE in another research project had shown that inducing thermal runaway in these cells through localized spot-heating required a larger heating element than the one used in the present setup.

The tests were conducted in October 2025 at RISE, Borås, Sweden.

2.4.2 The heating element

A Mica heating element supplied by Backer Calesco AB was used. Mica heaters consist of etched foil elements sandwiched between layers of mica. According to the supplier, the benefits of mica heaters include high power density, suitability for use in open-air assemblies, high operating temperatures, and fast warm-up times. The overall size of the heating element was 80 mm by 39 mm, and it provided a nominal heat level of 600 W at a 24 V current according to the supplier.

© RISE Research Institutes of Sweden

2.4.3 Fire test procedures

To establish benchmark data for the suppression tests, free-burn fire tests were conducted. In these tests, the entire ceiling of the test compartment was removed, which allowed the measurement of the heat release rate from the fires.

The free-burn results provided an indication of the temperature at which thermal runaway was triggered. Once thermal runaway occurred, the temperature propagation between cells was observed to be very rapid. Based on these findings, it was decided that carbon dioxide should be discharged when the surface temperature measured near the heating element approached the level associated with the onset of thermal runaway and not after the occurrence of thermal runaway.

For the fire suppression tests, a nominal carbon dioxide charge of 4.5 kg was selected to achieve a target atmosphere corresponding to approximately 11.5 % oxygen, equivalent to about 45 % carbon dioxide. However, the exact quantity of carbon dioxide discharged during each test could not be determined until after the test had been completed. According to the supplier, a full cylinder should contain a nominal 10 kg of carbon dioxide. Based on this information, the cylinder was placed on a load cell and discharged until its measured mass had decreased by 5.5 kg, leaving the intended 4.5 kg of carbon dioxide available for the test. Subsequent verification measurements, however, showed that the actual fill quantity of supposedly full cylinders could vary. As a result, the amount of carbon dioxide released during individual tests differed slightly from the desired value.

For the last test, Test 11 a full cylinder charge was used, resulting in a carbon dioxide concentration of approximately 70 %.

2.4.4 Results

Two initial free-burn fire tests were conducted using N-cells and V-cells, referred to as Test 1 and Test 2. Thermal runaway occurred after approximately 48 minutes for the N-cells (Test 1) and after about 10:30 (min:s) for the V-cells (Test 2). For these tests, no ceiling was installed in the test compartment.

For the V-cells in Test 2, thermal runaway of the first battery cell occurred at about 95 °C. Figure 11 shows the average surface temperature measured by the Plate Thermometers and the oxygen concentration inside the test compartment during this free-burn test.

© RISE Research Institutes of Sweden

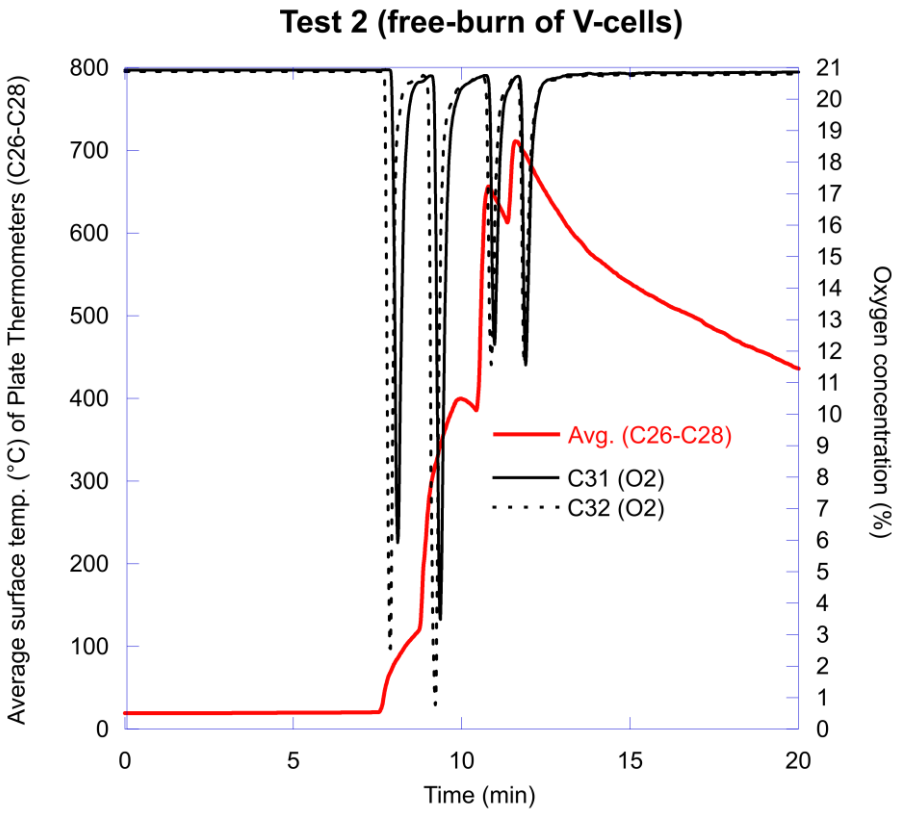

Figure 11 **Test 2:** The average surface temperature of the Plate Thermometers and the oxygen concentrations inside the test compartment during the free-burn test with the V-cells.

The total heat release rate measured in Test 2 clearly captured the intermittent involvement of the four prismatic V-cells, refer to Figure 12. Each involvement resulted in a distinct peak in the heat release rate, reaching approximately 200 kW. The time from the first peak to the last peak was about 228 seconds, or 03:48 (min:s), and the intervals between successive peaks were highly regular.

© RISE Research Institutes of Sweden

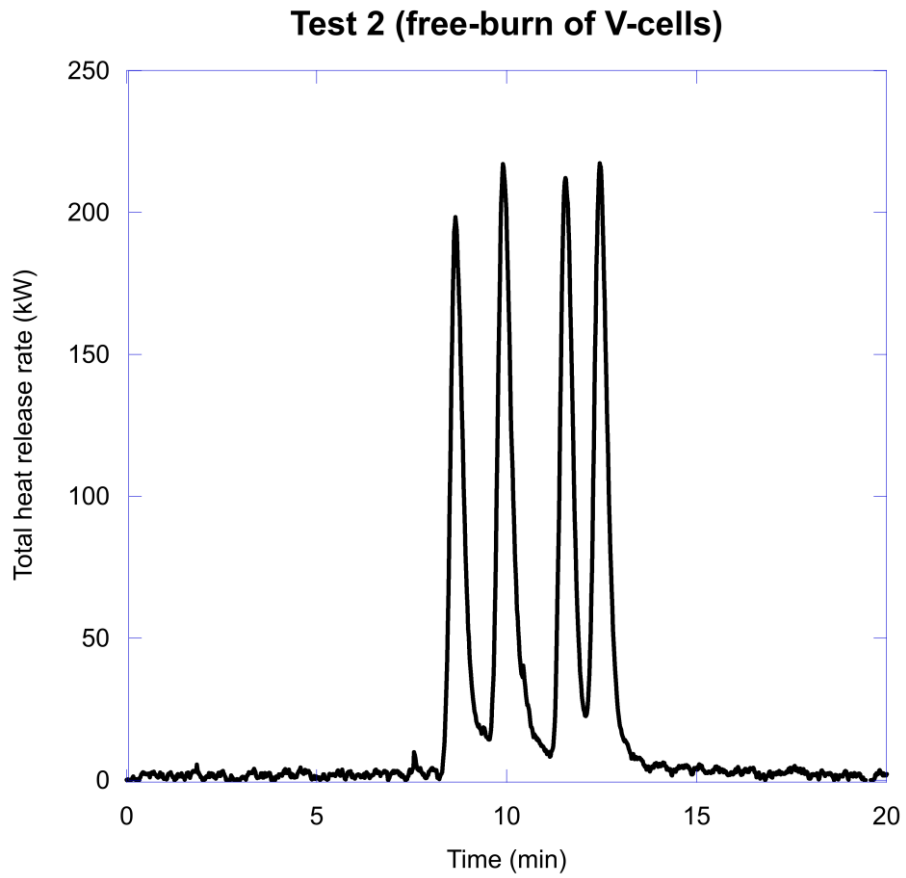

Figure 12 **Test 2:** The total heat release rate during the free-burn test with the V-cells.

The first fire suppression test was performed with V-cells (Test 3) without the ceiling installed in the test compartment. Carbon dioxide discharge was initiated when the surface temperature of the heated cell reached 50 °C. The discharge reduced the oxygen concentration inside the test compartment to approximately 12.0 %, refer to Figure 13. Thermal runaway of the first battery cell occurred at about 99 °C. However, once thermal runaway was initiated, the oxygen concentration increased rapidly, demonstrating that a ceiling was required to retain the carbon dioxide within the compartment. The average peak surface temperature of the Plate Thermometers was 766 °C, higher than that in the free-burn fire test (Test 2).

© RISE Research Institutes of Sweden

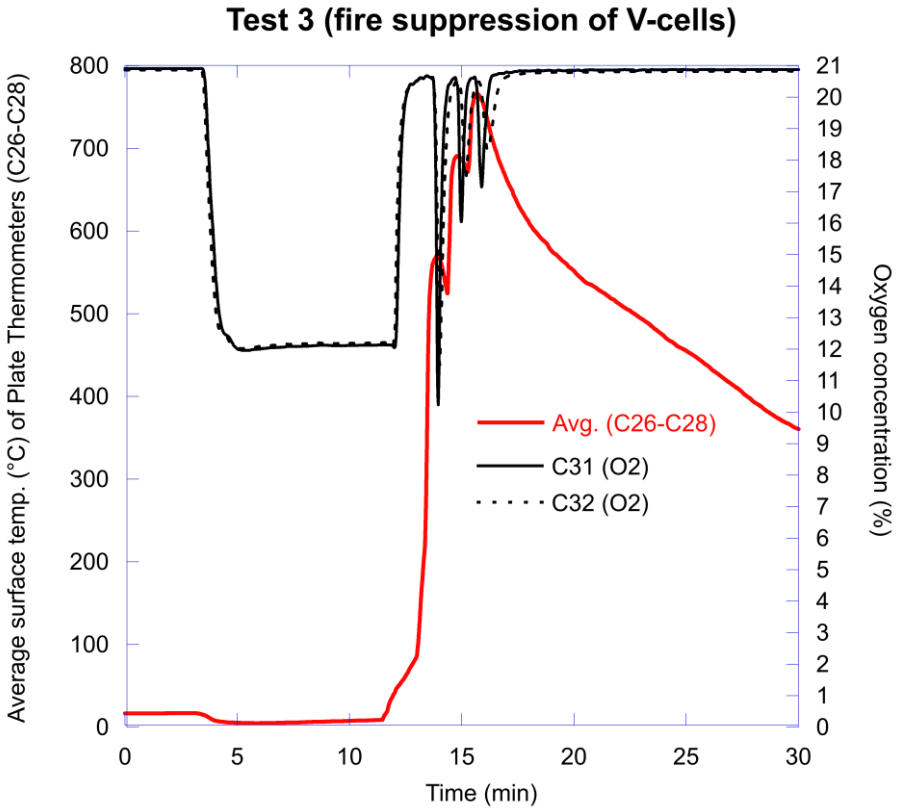

Figure 13 **Test 3:** The average surface temperature of the Plate Thermometers and the oxygen concentrations inside the test compartment during the first fire suppression test with the V-cells.

The total heat release rate measured in Test 3, refer to Figure 14, indicate that the low oxygen concentration could have had an influence on the peak heat release rate of the fire in the first battery cell. But as the combustion gases vented out of the compartment, no or marginal fire size reduction of the following cells are observed. The time from the first peak to the last peak was about 214 seconds, or 03:34 (min:s), a time similar to the free-burn fire test (Test 2).

© RISE Research Institutes of Sweden

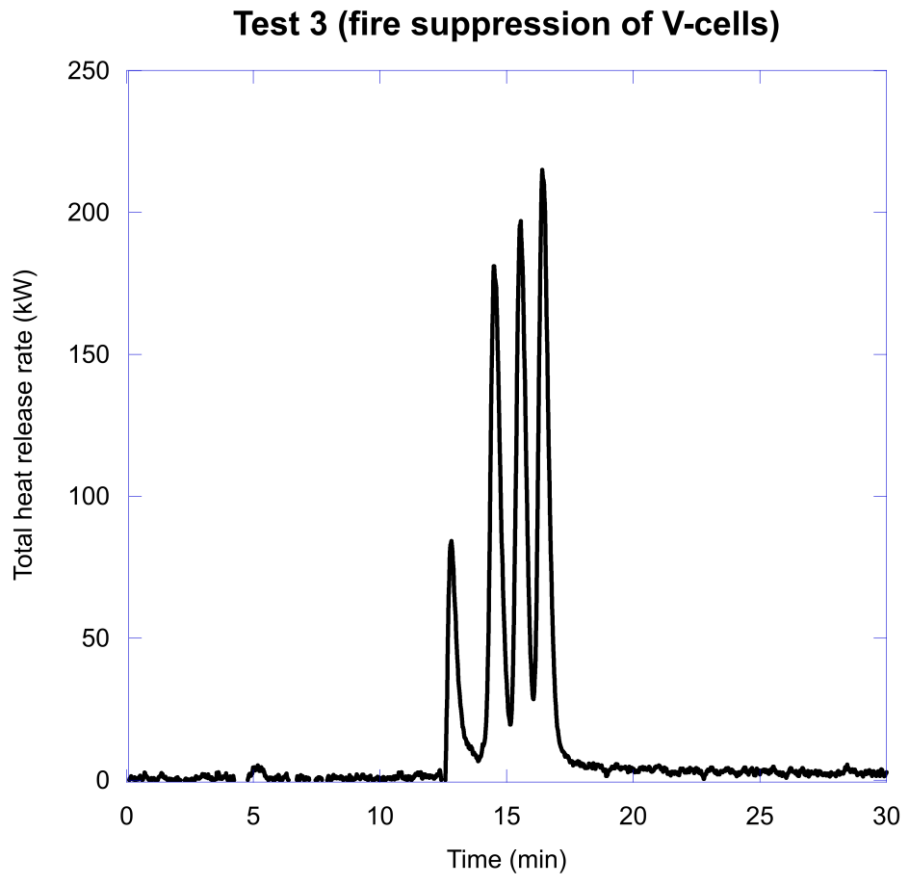

Figure 14 **Test 3:** The total heat release rate during the first fire suppression test with the V-cells.

A second suppression test with V-cells was conducted in Test 5, this time with the ceiling (with the pressure-relief hatch) installed. However, the heating element malfunctioned at approximately 95 °C, preventing the onset of thermal runaway. The test was therefore repeated as Test 6.

In Test 6, carbon dioxide was discharged when the surface temperature of the heated cell reached 60 °C. The discharge reduced the oxygen concentration inside the test compartment to approximately 10.0 %, refer to Figure 15. Thermal runaway of the first battery cell occurred at 164 °C, a temperature that was significantly higher than in the other two tests. At this point, the oxygen concentration inside the test compartment had increased to approximately 11.5 %, which corresponded to the target concentration equivalent to roughly 45 % carbon dioxide. The intermittent involvement of individual battery cells in the fire can be identified by short-term decreases in the oxygen concentration. The ceiling and hatch effectively prevented carbon dioxide from escaping the test compartment upwards. The gradual increase in oxygen concentration during the heating phase and following the burn-out of the cells is attributed to leakage through the lower sections of the test compartment. The average peak surface temperature measured by the Plate Thermometers was 656 °C, which was lower than that in the free-burn fire test (Test 2).

© RISE Research Institutes of Sweden

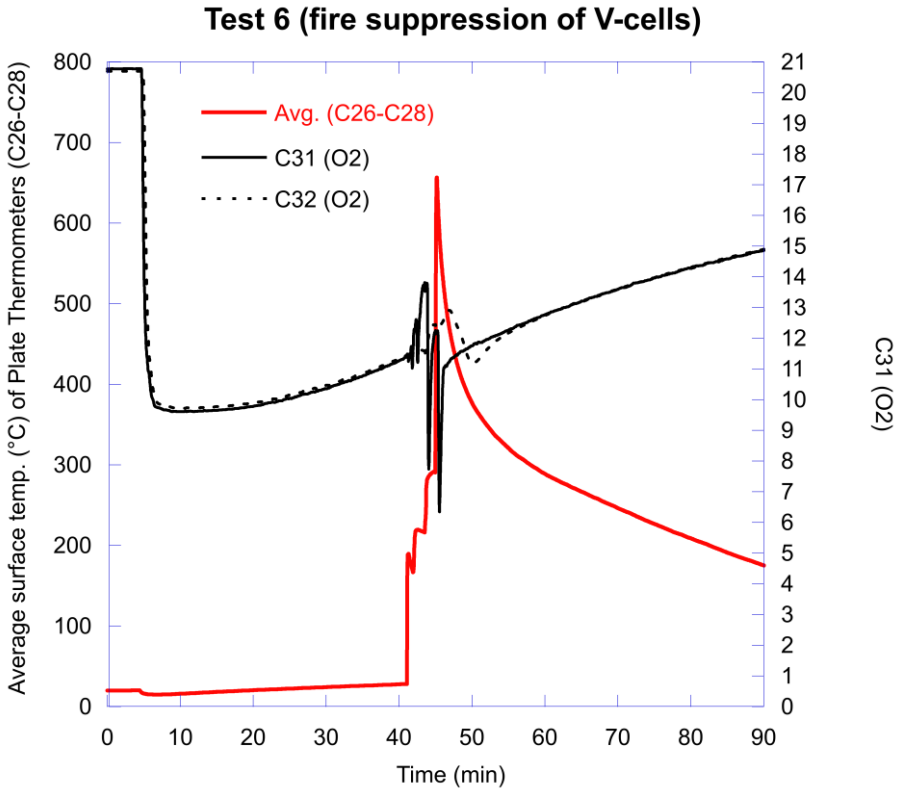

Figure 15 **Test 6:** The average surface temperature of the Plate Thermometers and the oxygen concentrations inside the test compartment during the second fire suppression test with the V-cells.

Based on the three tests involving the V-cells, the surface temperature measurements suggest that the presence of carbon dioxide in the test compartment (Test 6) may have contributed to a modest reduction in the peak surface temperature. The highest surface temperature recorded in Test 6 was 656 °C, compared with 711 °C in the corresponding free-burn test. In Test 3, where most of the carbon dioxide escaped the test compartment, the temperature was 766 °C.

The time elapsed between the initial recorded temperature increase, and the peak temperature was calculated for each test:

- Test 2 (free-burn): 258 seconds.
- Test 3: 254 seconds.
- Test 6: 244 seconds.

It could be anticipated that the carbon dioxide atmosphere would increase the time from the initial temperature rise to the peak temperature. However, the results do not support this expectation, as the measured times were comparable in all tests.

Two fire suppression tests (Tests 9 and 10) were conducted using N-cells, but in both cases the heating element failed at approximately 400 °C, prior to the onset of thermal runaway. Consequently, no comparative fire-suppression data could be obtained for the N-cells when inducing thermal runaway through localized spot-heating. It was concluded that the onset of thermal runaway in the N-cells and in the EVE-cells requires nail penetration.

© RISE Research Institutes of Sweden

Two free-burn fire tests were conducted with the cylindrical C-cells. In the first test (Test 4), the experiment was terminated after approximately 78 minutes because the temperatures did not reach sufficiently high levels and only one cell underwent thermal runaway. The remaining cells were unaffected. The test also demonstrated the need for a mechanically stronger containment cage to maintain closer contact between the cells. A reinforced cage was therefore used in the following tests with the cylindrical C-cells.

In the free-burn fire test of Test 8, the first audible "explosion" occurred approximately 2 minutes after heater activation. In total, six audible "explosions" were documented during the test. The minimum oxygen concentration was 19.5 %, refer to Figure 16, indicating that the fire had only a limited effect on the oxygen concentration within the test compartment. The average peak surface temperature measured by the Plate Thermometers was 265 °C.

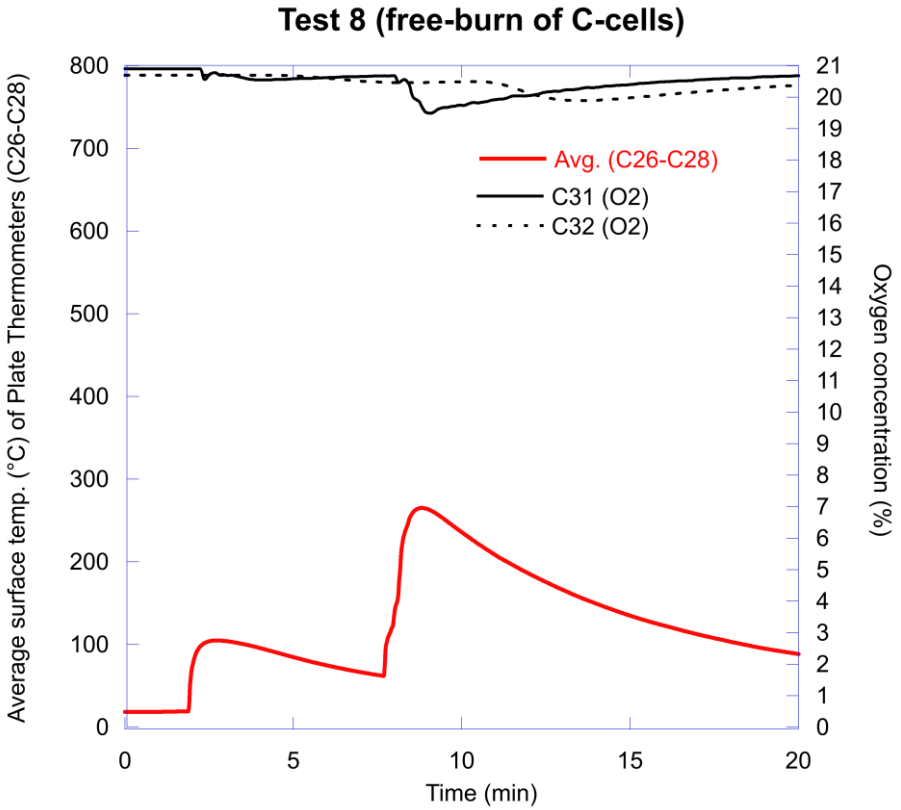

Figure 16 **Test 8:** The average surface temperature of the Plate Thermometers and the oxygen concentrations inside the test compartment during the free-burn test with the C-cells.

The fire did not generate any measurable heat release rate.

A fire suppression test was carried out in Test 7. As in the other fire suppression tests, carbon dioxide was pre-discharged into the test compartment during the heating stage. Based on the audible cues, several "explosions" were heard, and it was suspected that the reduced oxygen concentration in the compartment had only a limited effect on the severity of the fire. After the test, it was further concluded that all eight cylindrical battery cells had fully burned.

The discharge of carbon dioxide reduced the oxygen concentration within the test compartment to approximately 9.0 %, refer to Figure 17. The intermittent involvement

© RISE Research Institutes of Sweden

of individual battery cells in the fire can be identified from the surface temperature measurements of the Plate Thermometers; however, no corresponding fluctuations were observed in the oxygen concentration measurements that gradually increased over time due to leakage through the lower sections of the test compartment. The average surface temperature increased steadily throughout the test, and the average peak surface temperature measured by the Plate Thermometers was 175 °C, a lower temperature compared to the free-burn test (Test 8).

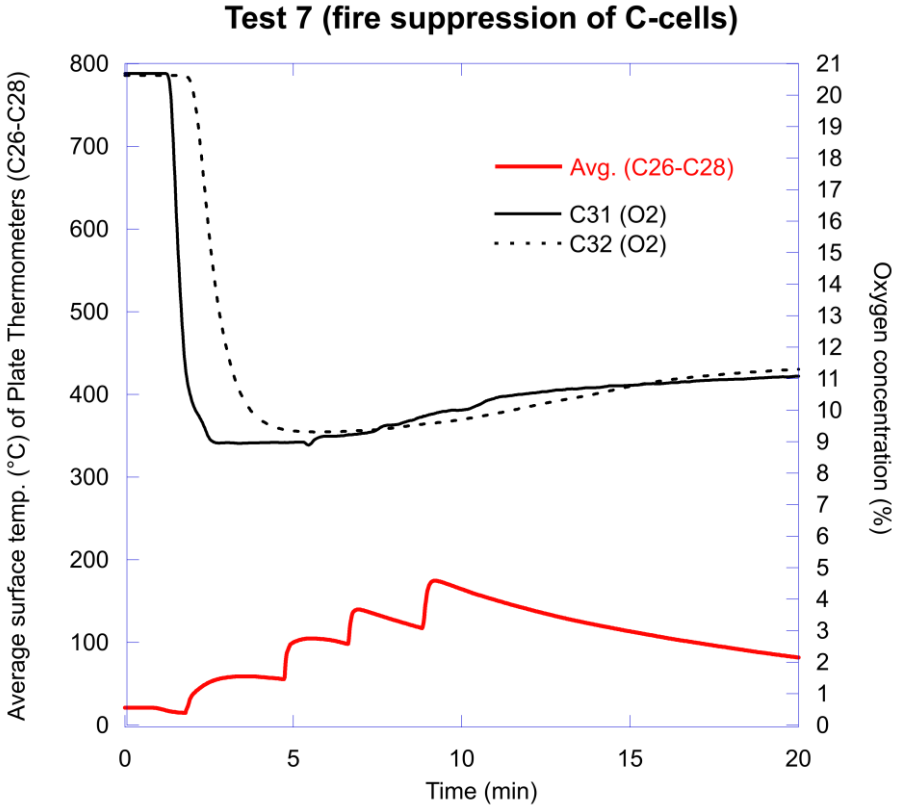

Figure 17 **Test 7:** The average surface temperature of the Plate Thermometers and the oxygen concentrations inside the test compartment during the first fire suppression test with the C-cells.

A second fire suppression test was conducted in Test 11. As in the previous fire suppression tests, carbon dioxide was pre-discharged into the test compartment during the heating stage; however, a larger quantity, of approximately 10 kg, was released. This reduced the oxygen concentration within the test compartment to approximately 6.5 %, refer to Figure 18. No intermittent cell involvement could be identified from the measurement data, and only two audible explosion events were observed. Furthermore, the oxygen concentration remained stable throughout the remainder of the test, with no discernible fluctuations indicating additional cell involvement. The average surface temperature increased steadily throughout the test, with the Plate Thermometers recording an average peak surface temperature of 124 °C, a lower temperature compared to the free-burn test (Test 8).

© RISE Research Institutes of Sweden

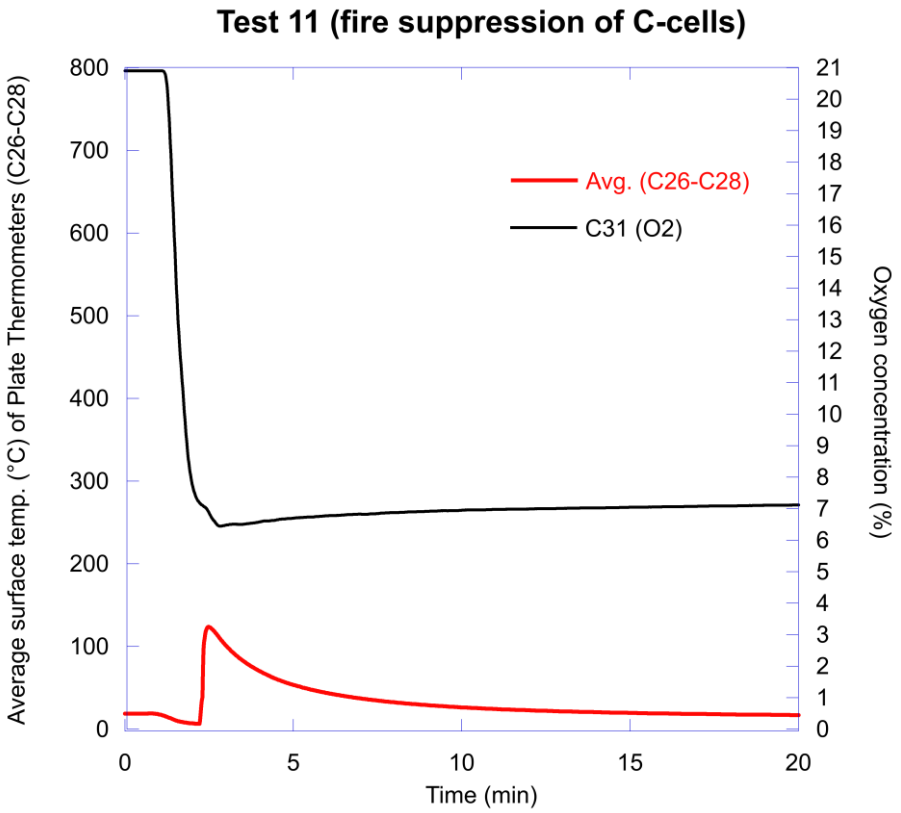

Figure 18 **Test 11:** The average surface temperature of the Plate Thermometers and the oxygen concentrations inside the test compartment during the second fire suppression test with the C-cells.

Based on the three tests involving the C-cells, the surface temperature measurements indicate that the presence of carbon dioxide in the test compartment resulted in a reduction in the peak surface temperature, from 265 °C, to 175 °C and 124 °C.

The time elapsed between the initial recorded temperature increase, and the peak temperature was calculated for all three tests:

- Test 8 (free-burn): 420 seconds.
- Test 7: 447 seconds.
- Test 11: 17 seconds.

The carbon dioxide atmosphere increased the time interval between the initial temperature rise and the peak temperature in Test 7 compared with the free-burn test (Test 8). In Test 11, the corresponding interval was considerably shorter, potentially indicating that the remaining six cylindrical cells did not experience violent thermal runaway. Taken together, these observations suggest that the carbon dioxide atmosphere contributed to a reduction in fire severity.

Table 6 summarizes the test conditions and results for the first series of tests. The average oxygen concentration during the period of thermal propagation was calculated to provide a representative measure of the oxygen concentration over an extended period, providing a representative value over the duration of the event.

© RISE Research Institutes of Sweden

Table 6 Summary of the test conditions and test results for the first series of tests, where thermal runaway was initiated using a heating element.

Test	Type of cell	Amount of CO2 (kg)	Average peak surface temperature (°C)	Average oxygen concentration during thermal propagation (%)	Elapsed time from nail penetration to peak surface temperature (s)
2	V-cells	Free-burn	711 °C	18.2 %	258 s
3*	V-cells	6.3 kg	766 °C	19.3 %	254 s
6	V-cells	5.6 kg	656 °C	12,7 %	244 s
8	C-cells	Free-burn	265 °C	20.4 %	420 s
7	C-cells	6.3 kg	175 °C	9.8 %	447 s
11	C-cells	10 kg	124 °C	6.7 %	17 s

*) No ceiling was installed during this fire suppression test, resulting in only a limited reduction in oxygen concentration.

The fire in the battery cells influenced the oxygen concentration in the test compartment through two mechanisms. First, the combustion process reduced the oxygen concentration through the consumption of oxygen and the generation of combustion gases. Second, the pressure rise caused by the fire resulted in carbon dioxide being expelled through the compartment's pressure-relief hatch in the ceiling. In addition, the amount of carbon dioxide released during individual tests differed slightly from the nominal value, as discussed in Section 2.4.3. Consequently, maintaining precise control of the oxygen concentration during the tests was challenging.

For the free-burn fire test with the V-cells (Test 2), the fire in the battery cells had a measurable but not significant effect on the oxygen concentration within the test compartment. In Test 3, the absence of a ceiling resulted in only a limited reduction in oxygen concentration. The average oxygen concentration in Test 6 was, however, relatively close to the target value of 11.5 %.

The fires in the cylindrical C-cells were considerably less severe than those involving the V-cells, and the impact of the fire itself on the oxygen concentration was correspondingly less significant. This made it possible to conduct a free-burn test (Test 8), in which the reduction in oxygen concentration within the test compartment was limited. In the first fire suppression test (Test 7), the average oxygen concentration was reasonably close to the target value of 11.5 %. In the second fire suppression test, a larger quantity of carbon dioxide was intentionally discharged, resulting in an oxygen concentration close to the expected value.

The cylindrical cells were significantly smaller than the prismatic cells and contained only a fraction of the stored energy, resulting in less severe fires at the individual-cell level. In addition, the arrangement of cylindrical cells provided a considerably smaller contact area between adjacent cells, reducing the potential for conductive heat transfer and thermal propagation within the array. These differences may partly explain the

© RISE Research Institutes of Sweden

greater reduction in overall fire severity observed in the cylindrical-cell array when carbon dioxide was applied.

2.5 Second series of tests

2.5.1 General

These tests included the prismatic N-cells, V-cells and EVE-cells, while the cylindrical C-cells were not part of the test series.

The tests were conducted in February 2026 at RISE, Borås, Sweden.

2.5.2 The nail penetration equipment

Ignition was initiated using nail penetration. A pneumatic cylinder (compressed air) was used to drive a 3 mm diameter steel nail into the long side of one of the outermost cells. As soon as the nail breached the cell casing, the compressed-air supply was disconnected to prevent unnecessary air from entering the test compartment. The nail penetrated approximately 30 mm into the cell(s). Figure 19 shows the arrangement for the nail penetration.

Figure 19 The principal arrangement for nail penetration, at the long side of the outermost prismatic cell. The Plate Thermometers positioned above (facing the top) and at the sides (facing each of the short sides) are not installed in the photos.

2.5.3 Fire test procedures

To establish benchmark data for the fire suppression tests, free-burn fire tests were conducted. During these tests, the ceiling hatch remained open to allow combustion gases to vent and to enable measurement of the heat release rate.

Despite several attempts, ignition of the EVE cells could not be achieved. Between the first (Test 4) and second (Test 5) tests, the nail penetration location was adjusted; however, no ignition occurred in either test. Notably, unlike the other battery cells tested, the EVE cells were of the lithium iron phosphate (LFP) chemistry.

Once thermal runaway was initiated in the free-burn tests, temperature propagation between adjacent N- and V-cells was found to be extremely rapid. Based on these

© RISE Research Institutes of Sweden

findings, it was decided to pre-discharge carbon dioxide prior to nail penetration during the fire suppression tests, as thermal runaway occurred immediately following penetration.

For the fire suppression tests, two nominal carbon dioxide quantities were used: 4.5 kg and 10 kg. The former corresponded to the amount of carbon dioxide required to achieve the target concentration of 45 % (about 11.5 % oxygen), whereas the latter represented a full cylinder charge, resulting in a carbon dioxide concentration of approximately 70 % (about 6.3 % oxygen). In all fire suppression tests, the ceiling hatch remained closed; however, it was designed to open in response to overpressure within the test compartment.

The test procedure was as follows. First, the carbon dioxide system was activated, and the specified quantity of carbon dioxide was discharged into the test compartment. The amount discharged was determined from the measured weight loss of the cylinder. This method provided a more accurate determination of the carbon dioxide quantity than that used in the first series of tests (see Section 2.4.3). The discharge time was approximately 90 seconds. The oxygen concentration was then measured and documented. Thermal runaway was subsequently initiated by nail penetration at a predetermined clock time (time “zero” in the measurement graphs). Immediately thereafter, the compressed-air coupling at the connection point in the fire hall was disconnected to depressurize the pneumatic nail-penetration valve.

2.5.4 Results

One free-burn fire test was conducted using N-cells, designated Test 1. As noted previously, the ceiling hatch remained open throughout the test to enable measurement of the heat release rate. Despite the open hatch, the accumulation of combustion gases gradually reduced the oxygen concentration within the test compartment. Following thermal runaway of the fourth battery cell, the oxygen concentration reached a minimum value of approximately 7.6 %, refer to Figure 20.

Each thermal runaway event generated substantial turbulence within the compartment, resulting in noticeable fluctuations in the measured oxygen concentration. The average oxygen concentration during the thermal propagation in the cells was about 11.9 %. The average peak surface temperature recorded by the Plate Thermometers was 501 °C.

© RISE Research Institutes of Sweden

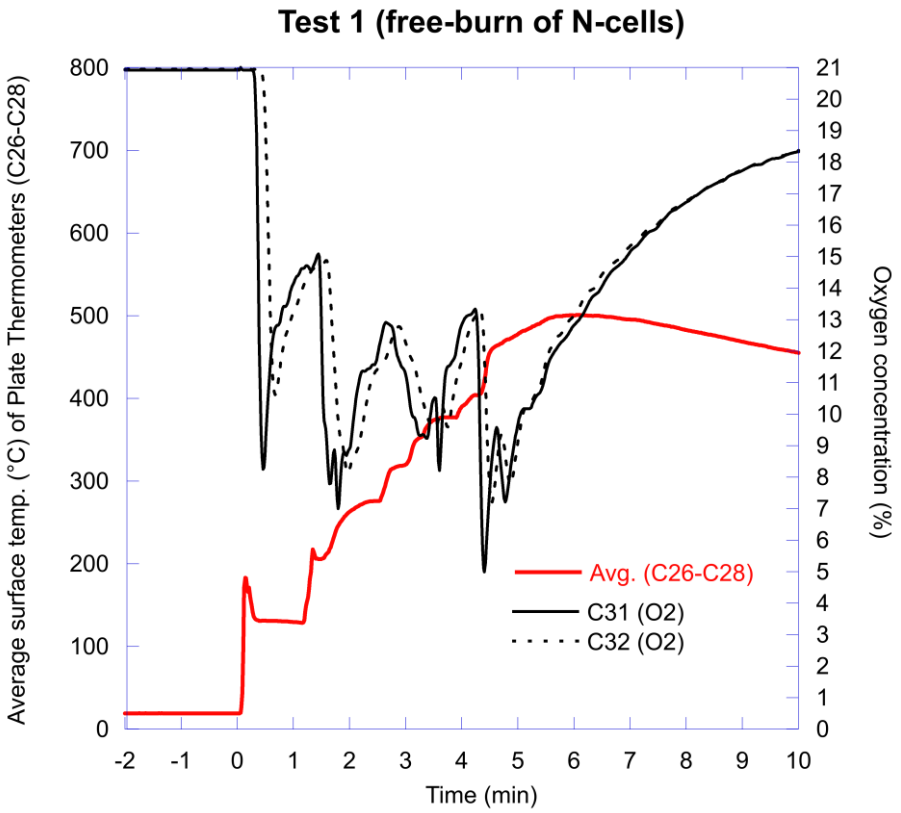

Figure 20 **Test 1:** The average surface temperature of the Plate Thermometers and the oxygen concentrations inside the test compartment during the free-burn test with the N-cells.

The total heat release rate measured in Test 1 clearly captured the intermittent involvement of the four prismatic N-cells, refer to Figure 21. Each involvement resulted in a distinct peak in the heat release rate, reaching approximately 100 kW. The time from the first peak to the last peak was about 250 seconds, or 04:10 (min:s), and the intervals between successive peaks were highly regular.

© RISE Research Institutes of Sweden

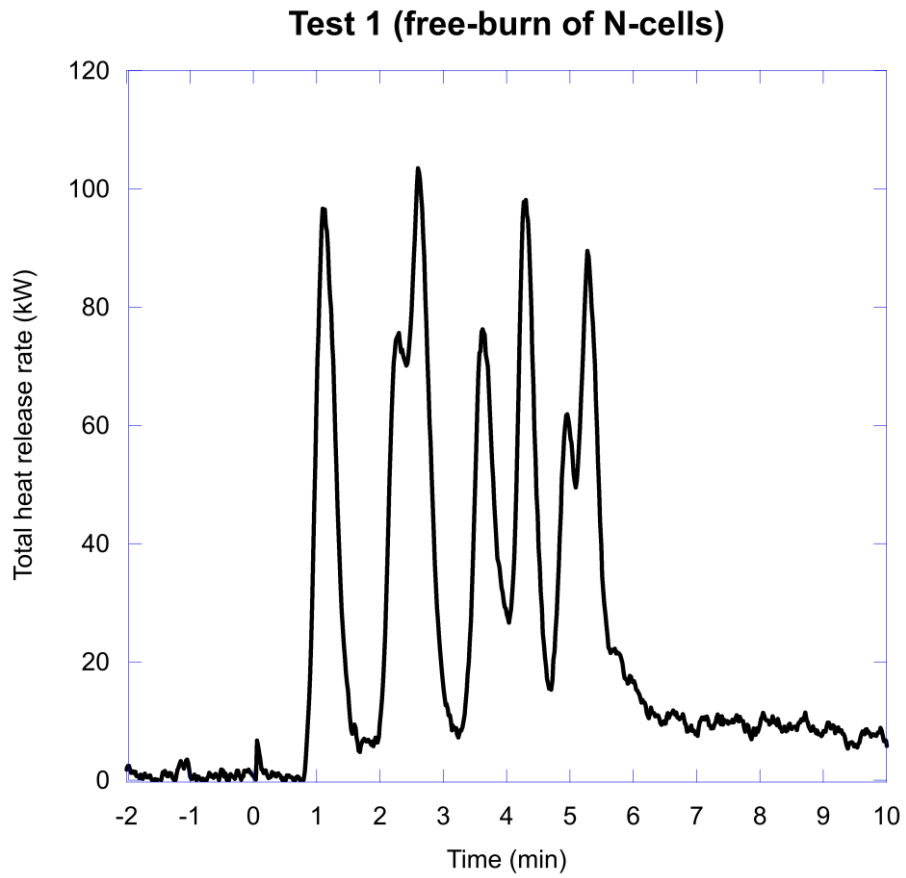

Figure 21 **Test 1:** The total heat release rate during the free-burn test with the N-cells.

Test 2 was conducted using N-cells with a pre-discharge of a nominal 4.5 kg of carbon dioxide. This reduced the oxygen concentration within the test compartment to approximately 11.4 % prior to nail penetration, refer to Figure 22. The thermal runaway and subsequent fire involvement of the first and second battery cells had only a limited effect on the oxygen concentration. However, involvement of the third and fourth cells caused a further reduction, resulting in a minimum oxygen concentration of 4.4 % and an average oxygen concentration during the thermal propagation in the cells of about 9.9 %. The average peak surface temperature recorded by the Plate Thermometers was 533 °C, which was higher than in the free-burn test (Test 1).

© RISE Research Institutes of Sweden

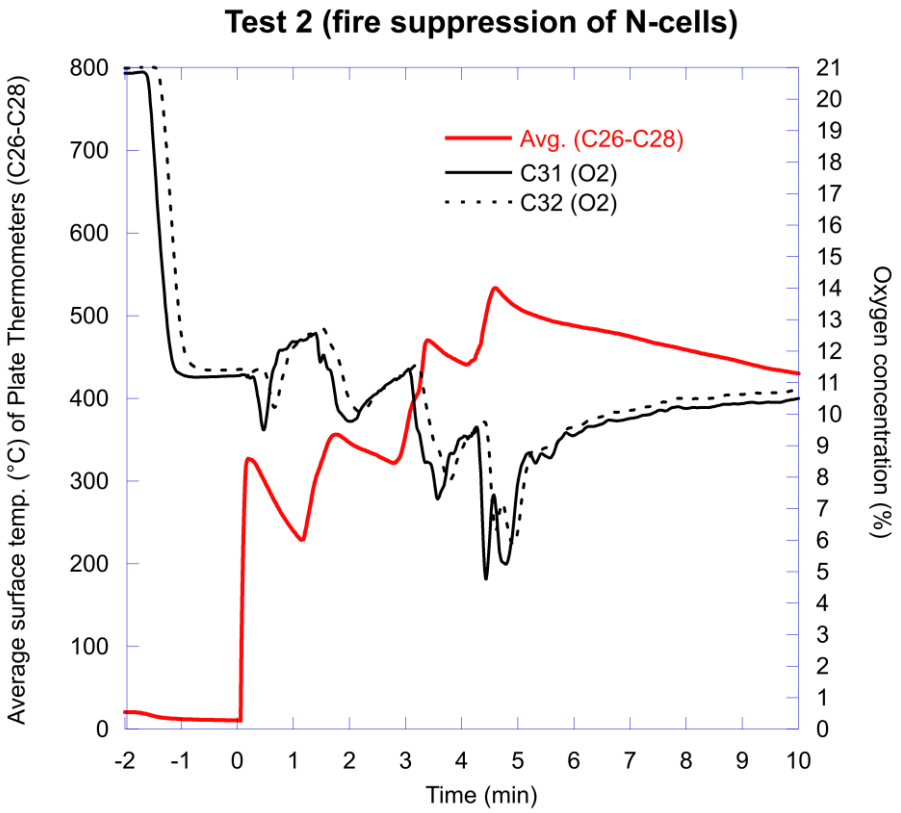

Figure 22 **Test 2:** The average surface temperature of the Plate Thermometers and the oxygen concentrations inside the test compartment during the first fire suppression test with the N-cells.

© RISE Research Institutes of Sweden

Test 3 was conducted using N-cells with a pre-discharge of a nominal 10 kg of carbon dioxide. This reduced the oxygen concentration within the test compartment to approximately 6.1 % prior to nail penetration, refer to Figure 23. The thermal runaway and subsequent fire involvement of the first cell had only a limited effect on the oxygen concentration. However, involvement of the second, third, and fourth cells resulted in fluctuations and an overall increase in the measured oxygen concentration. The minimum oxygen concentration was 7.5 %, and the average oxygen concentration during the thermal propagation in the cells was about 8.9 %. The average peak surface temperature recorded by the Plate Thermometers was 657 °C, which was higher than in the free-burn test (Test 1).

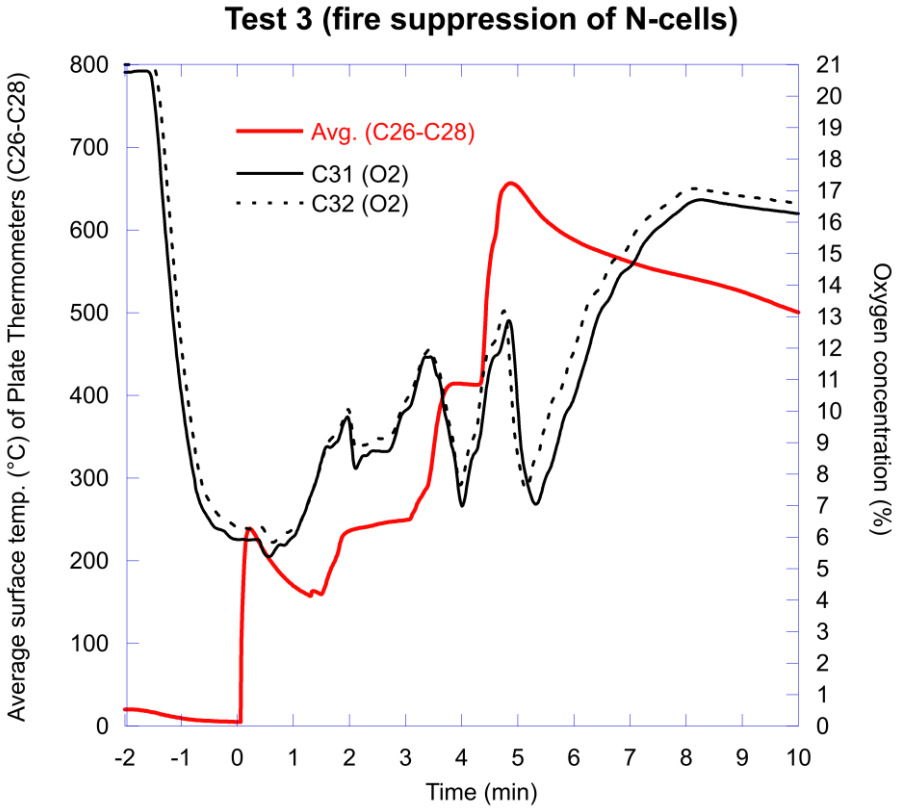

Figure 23 **Test 3:** The average surface temperature of the Plate Thermometers and the oxygen concentrations inside the test compartment during the second fire suppression test with the N-cells.

Based on the three tests with the V-cells, the surface temperature measurements indicate that the presence of carbon dioxide in the test compartment did not contribute to a decrease of the peak surface temperature. In fact, the peak temperatures measured in both Test 2 and Test 3 was higher than that recorded in the free-burn test of Test 1.

The time elapsed between the nail penetration, and the peak surface temperature was calculated for each test:

- Test 1 (free-burn): 355 seconds.
- Test 2: 275 seconds.
- Test 3: 294 seconds.

© RISE Research Institutes of Sweden

A carbon dioxide atmosphere would be expected to increase the time between the onset of the temperature rise and the peak temperature. However, this trend was not observed. The intervals measured in Tests 2 and 3 were similar, whereas the free-burn test in Test 1 exhibited the longest duration.

In the free-burn fire test (Test 6) with the V-cells, the combustion gases that was generated during the intermittent involvement of the battery cells gradually reduced the oxygen concentration inside the test compartment, reaching a minimum of approximately 9.7 %, refer to Figure 24. The average oxygen concentration during the thermal propagation in the cells was about 13.1 %. The average peak surface temperature recorded by the Plate Thermometers was 468 °C.

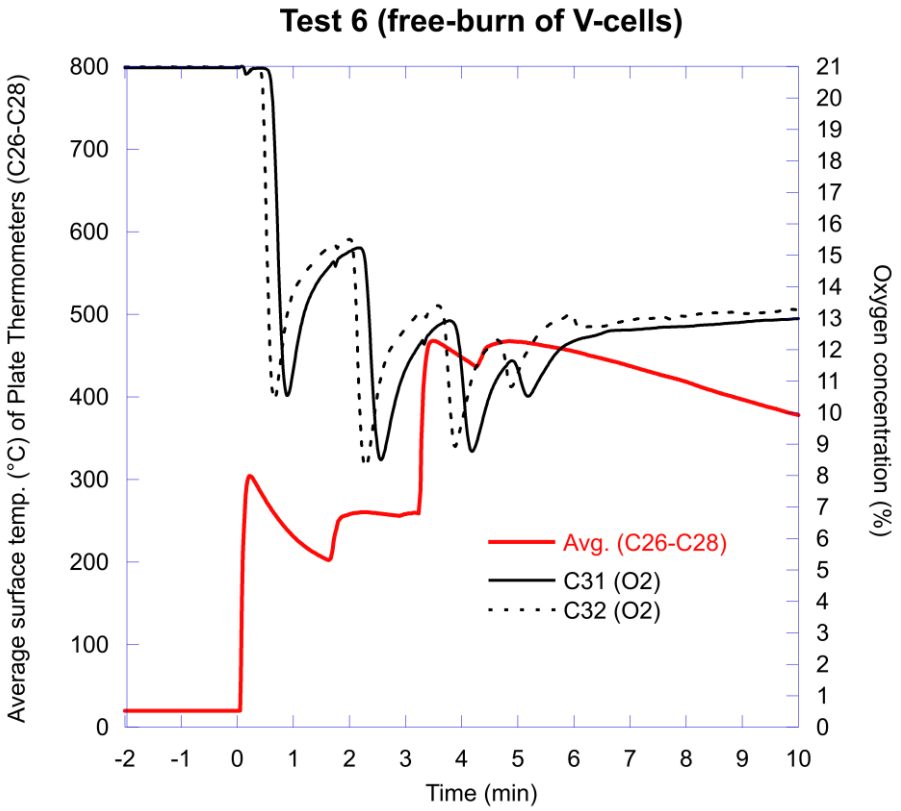

Figure 24 **Test 6:** The average surface temperature of the Plate Thermometers and the oxygen concentrations inside the test compartment during the free-burn test with the V-cells.

The total heat release rate measured in Test 6 clearly captured the intermittent involvement of the four prismatic V-cells, refer to Figure 25. Each involvement resulted in a distinct peak in the heat release rate, where the involvement of the third battery cell resulted in a peak of almost 180 kW. The time from the first peak to the last peak was about 253 seconds, or 04:13 (min:s), and the intervals between successive peaks were highly regular.

© RISE Research Institutes of Sweden

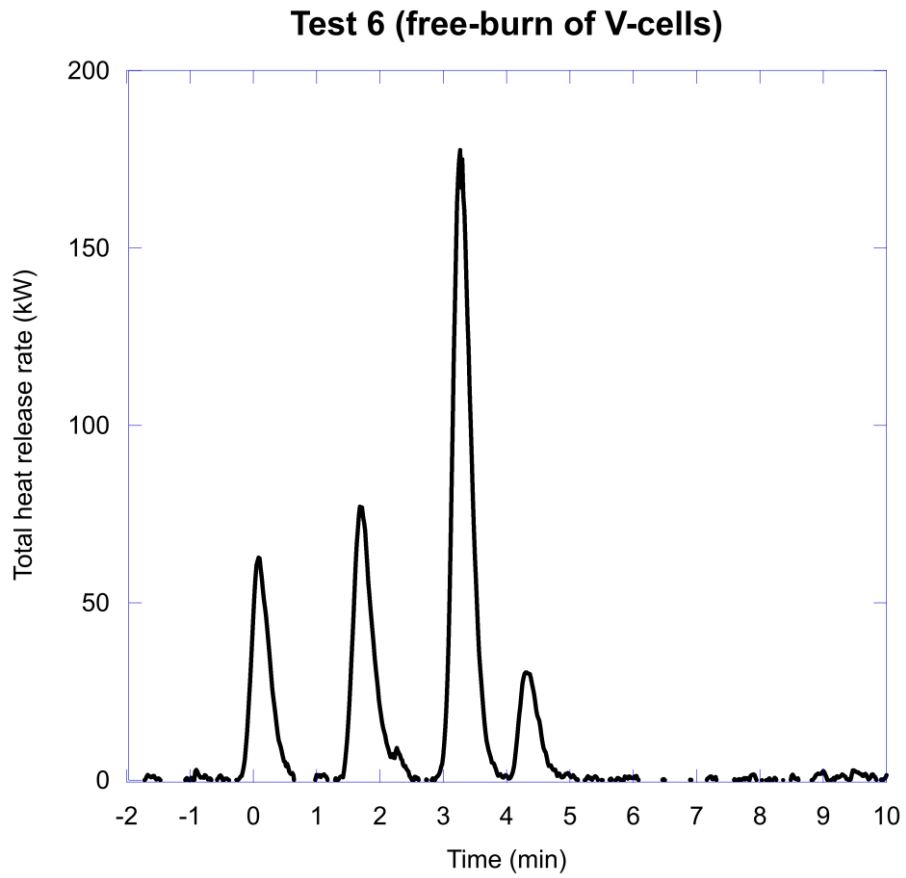

Figure 25 **Test 6:** The total heat release rate during the free-burn test with the V-cells.

In the first fire suppression test (Test 7) with the V-cells, 4.5 kg of carbon dioxide was pre-discharged, and the initial oxygen concentration was approximately 11.4 %, refer to Figure 26. When the first cell entered thermal runaway, the combustion gases displaced part of the carbon dioxide atmosphere, causing the oxygen concentration to increase. The involvement of the second and fourth cells temporarily reduced the oxygen concentration, whereas the fire in the third cell had only a minor impact on the overall oxygen level. The minimum oxygen concentration recorded during the test was 5.8 %, and the average oxygen concentration during the thermal propagation in the cells was about 11.4 %, which was close to the desired level. The average peak surface temperature recorded by the Plate Thermometers was 476 °C, higher than in the free-burn test (Test 6).

© RISE Research Institutes of Sweden

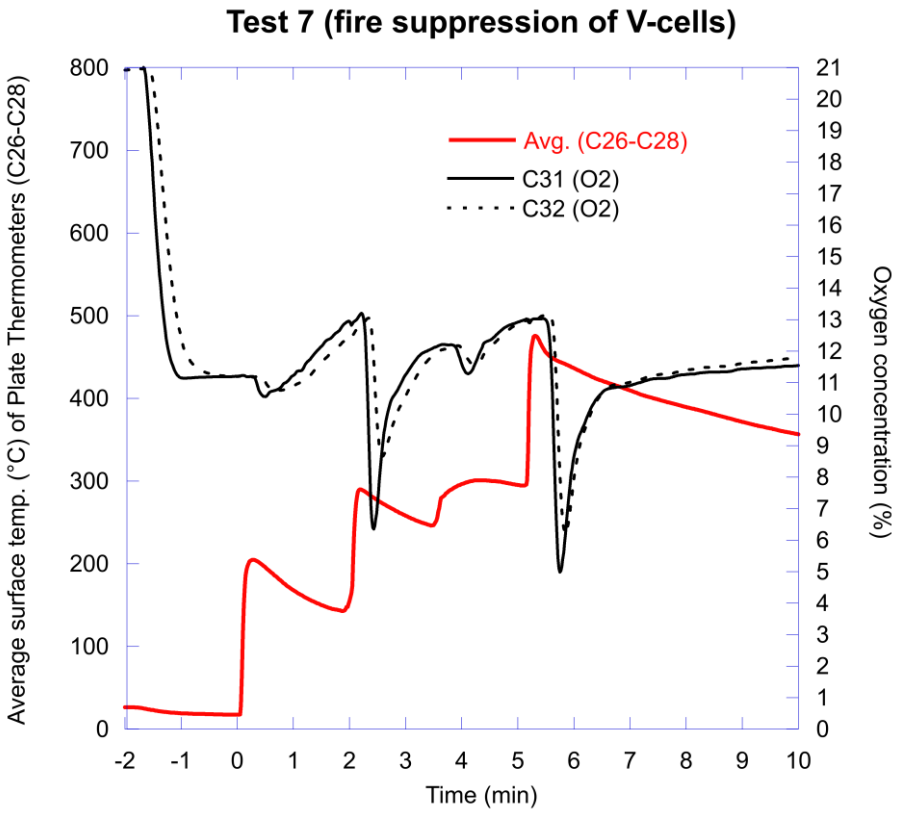

Figure 26 **Test 7:** The average surface temperature of the Plate Thermometers and the oxygen concentrations inside the test compartment during the first fire suppression test with the V-cells.

In the second fire suppression test (Test 8) with the V-cells, which included a pre-discharge of 10 kg of carbon dioxide, the initial oxygen concentration was approximately 6.1 %, refer to Figure 27. When the cells entered thermal runaway, the oxygen concentration increased rather than decreased, and the average oxygen concentration during the thermal propagation in the cells was about 9.6 %. This indicates that the combustion gases displaced part of the carbon dioxide atmosphere, resulting in a net increase in the measured oxygen concentration. The average peak surface temperature recorded by the Plate Thermometers was 532 °C, higher than in the free-burn test (Test 6).

© RISE Research Institutes of Sweden

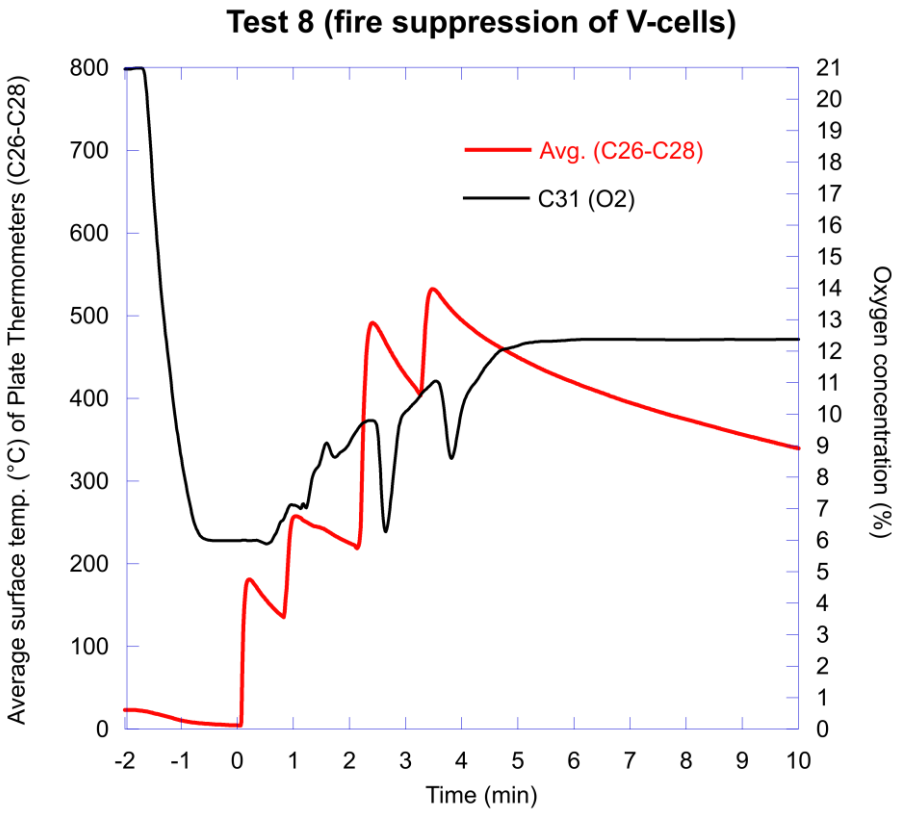

Figure 27 **Tests 8:** The average surface temperature of the Plate Thermometers and the oxygen concentration (the oxygen measurement point of C32 malfunctioned) inside the test compartment during the second fire suppression test with the V-cells.

Based on the three tests with the V-cells, the surface temperature measurements indicate that the presence of carbon dioxide in the test compartment did not contribute to a decrease of the peak surface temperature. In fact, the peak temperatures measured in both Test 7 (476 °C) and Test 8 (532 °C) was higher than that recorded in the free-burn test of Test 6 (468 °C).

The time elapsed between the nail penetration, and the peak surface temperature was calculated for each test:

- Test 6 (free-burn): 289 seconds.
- Test 7: 319 seconds.
- Test 8: 208 seconds.

It could be expected that a carbon dioxide atmosphere would increase the time between the initial temperature rise and the peak temperature. However, the results do not support this hypothesis, as the measured duration was relatively similar in Test 7 and shorter in Test 8.

Table 7 summarizes the test conditions and results for the second series of tests. The average oxygen concentration during the period of thermal propagation was calculated to provide a representative measure of the oxygen concentration over an extended period, providing a representative value over the duration of the event.

© RISE Research Institutes of Sweden

Table 7 Summary of the test conditions and test results for the second series of tests, where thermal runaway was initiated using nail penetration.

Test	Type of cell	Amount of CO_2 (kg)	Average peak surface temperature (°C)	Average oxygen concentration during thermal propagation (%)	Elapsed time from nail penetration to peak surface temperature (s)
1	N-cells	Free-burn	501 °C	11.9 %	355 s
2	N-cells	4.5 kg	533 °C	9.9 %	275 s
3	N-cells	10 kg	657 °C	8.9 %	294 s
6	V-cells	Free-burn	468 °C	13.1 %	289 s
7	V-cells	4.5 kg	476 °C	11.4 %	319 s
8	V-cell	10 kg	532 °C	9.6 %	208 s

For the second series of tests, the procedures enabled a more accurate determination of the quantity of carbon dioxide discharged. Two nominal carbon dioxide quantities were used: 4.5 kg, corresponding to an oxygen concentration of approximately 11.5 % in the absence of a fire, and 10 kg, corresponding to an oxygen concentration of approximately 6.3 %. However, the fire itself influenced the oxygen concentration through both oxygen consumption and the pressure rise generated by the fire, which caused carbon dioxide to be vented from the test compartment. Consequently, maintaining precise control of the oxygen concentration during the tests remained challenging.

Nevertheless, the tests provided a useful basis for comparing the fire severity of the two cell types at three different oxygen concentration levels. However, the oxygen concentration during the free-burn benchmark tests could not be controlled precisely and remained substantially below ambient levels during thermal propagation. This occurred despite the ceiling hatch being kept open to allow the venting of combustion gases from the test compartment. As a result, the benchmark tests may underestimate the fire suppression effectiveness and flame-cooling effects of carbon dioxide, since the fires were influenced by oxygen-depleted conditions.

© RISE Research Institutes of Sweden

3 Discussion

The objective of the present study was to investigate whether a carbon dioxide atmosphere could reduce the severity of lithium-ion battery fires and thermal runaway propagation in different cell types. A major challenge throughout the study was controlling the oxygen concentration. In both test series, the fires themselves influenced the atmosphere inside the test compartment. Oxygen was consumed during combustion, while fire-induced pressure increases caused combustion gases and carbon dioxide to be displaced through the pressure-relief hatch. Consequently, the actual oxygen concentrations during thermal propagation differed from the nominal concentrations established prior to ignition. This effect was particularly evident in the second test series, where several tests showed increasing oxygen concentrations following thermal runaway despite an initially high carbon dioxide concentration. Therefore, the test results should be interpreted as representing a range of oxygen concentrations rather than precisely controlled atmospheric conditions.

The first test series showed indications that carbon dioxide could reduce the severity of fires involving both prismatic V-cells and cylindrical C-cells. For the V-cells, the lowest average peak Plate Thermometer temperature was measured in Test 6, where the average oxygen concentration during thermal propagation was approximately 12.7 %. The corresponding peak temperature was about 8 % lower than in the free-burn test. However, the reduction was modest, and no corresponding increase in the time required for thermal propagation between cells was observed. The duration from the first temperature rise to peak temperature remained essentially unchanged. These observations suggest that while carbon dioxide may have reduced the intensity of flaming combustion, it did not significantly delay thermal runaway propagation between the cells.

The effect of carbon dioxide was considerably more pronounced for the cylindrical C-cells. Compared with the free-burn benchmark test, the average peak Plate Thermometer temperature decreased from 265 °C to 175 °C with approximately 10 % oxygen and further to 124 °C with approximately 7 % oxygen. These results indicate that the carbon dioxide atmosphere substantially reduced the severity of the fire and may have limited the extent of thermal runaway propagation.

The difference in response between the V-cells and the C-cells is likely related to the physical characteristics of the cell assemblies. The cylindrical cells were substantially smaller and contained only a fraction of the energy stored in the prismatic cells. In addition, the contact area between neighbouring cylindrical cells was significantly smaller, reducing conductive heat transfer and making thermal propagation more dependent on external flaming and radiative heating. Since carbon dioxide suppresses flaming combustion and reduces oxygen availability, it could be expected to have a greater influence on this type of propagation mechanism. In contrast, the large prismatic cells were mounted in direct contact with each other, creating favourable conditions for conductive heat transfer. Once thermal runaway was initiated, heat transfer between adjacent cells may therefore have been sufficiently strong to sustain propagation even at reduced oxygen concentrations.

© RISE Research Institutes of Sweden

The second test series produced different results. For both N-cells and V-cells, no consistent reduction in peak temperatures was observed following the introduction of carbon dioxide. In fact, the highest temperatures were measured in some of the suppression tests. Similarly, the time from nail penetration to peak temperature did not increase with decreasing oxygen concentration. At first sight, these observations may appear inconsistent with the results obtained during the first test series. However, an important difference was the initiation method. Nail penetration caused immediate and violent internal failure of the cell, rapidly triggering thermal runaway. Under such conditions, much of the energy release originates from exothermic reactions within the cell itself, which are largely independent of the external oxygen concentration. Carbon dioxide can suppress secondary flaming combustion, but it cannot prevent the internal decomposition reactions that drive thermal runaway once they have started. Consequently, its influence on thermal propagation may be limited when ignition is initiated by direct cell penetration.

Another important observation is that the free-burn benchmark tests in the second test series were not conducted under ambient atmospheric conditions. Despite the ceiling hatch being open, combustion gases accumulated inside the test compartment and reduced the oxygen concentration substantially below ambient levels. Average oxygen concentrations during thermal propagation ranged from approximately 12 % to 13 %, values that were not dramatically different from those measured in several of the suppression tests. As a result, the differences between the benchmark and suppression conditions were smaller than originally intended. This may partly explain why only limited suppression effects were observed in the second series and suggests that the effectiveness of carbon dioxide may have been underestimated.

Overall, the results indicate that carbon dioxide can reduce fire severity in lithium-ion battery fires, particularly for smaller cylindrical cells where thermal propagation appears to depend more strongly on flaming combustion and external heat transfer. For larger prismatic NMC cells, particularly when thermal runaway was initiated by nail penetration, the influence of carbon dioxide was much less pronounced. The findings therefore suggest that the effectiveness of carbon dioxide depends not only on the achieved oxygen concentration but also on the characteristics of the battery cells and the mechanisms governing thermal runaway propagation. Further testing with improved atmospheric control and direct measurements of propagation between individual cells would be valuable for quantifying these effects more accurately.

© RISE Research Institutes of Sweden

4 Conclusion

This study examined how carbon dioxide affects the severity of lithium-ion battery fires and thermal runaway propagation across different cell types and initiation methods. The results show that its effectiveness depends strongly on both battery design and the mechanism that triggers thermal runaway.

When thermal runaway was initiated by external heating, carbon dioxide reduced fire severity, particularly for cylindrical C-cells. This suggests that a carbon dioxide atmosphere can suppress flaming combustion and help limit propagation when heat transfer is driven mainly by external flames and radiation. For the larger prismatic V-cells, the effect was less pronounced, with lower peak temperatures but no clear delay in propagation.

When thermal runaway was triggered by nail penetration, carbon dioxide had little measurable impact. Neither the N-cells nor the V-cells showed consistent reductions in peak temperatures or delays in propagation. These results indicate that thermal runaway caused by severe internal damage is dominated by internal exothermic reactions that are largely unaffected by the surrounding atmosphere. In such cases, carbon dioxide may reduce secondary flaming but is unlikely to prevent propagation.

The results from this study indicate that carbon dioxide can reduce the severity of lithium-ion battery fires, but its effectiveness depends on cell design, heat-transfer mechanisms, and the initiation method. It appears most beneficial when flaming combustion plays a significant role in propagation and less effective when propagation is driven primarily by internal heat transfer. Further studies with improved atmospheric control and larger test matrices are needed to better define the conditions under which carbon dioxide can effectively mitigate lithium-ion battery fires.

© RISE Research Institutes of Sweden

Through our international collaboration programmes with academia, industry, and the public sector, we ensure the competitiveness of the Swedish business community on an international level and contribute to a sustainable society. Our 2,800 employees support and promote all manner of innovative processes, and our roughly 100 testbeds and demonstration facilities are instrumental in developing the future-proofing of products, technologies, and services. RISE Research Institutes of Sweden is fully owned by the Swedish state.

I internationell samverkan med akademi, näringsliv och offentlig sektor bidrar vi till ett konkurrenskraftigt näringsliv och ett hållbart samhälle. RISE 2 800 medarbetare driver och stöder alla typer av innovationsprocesser. Vi erbjuder ett 100-tal test- och demonstrationsmiljöer för framtidssäkra produkter, tekniker och tjänster. RISE Research Institutes of Sweden ägs av svenska staten.

RISE Research Institutes of Sweden AB Box 857, 501 15 BORÅS, SWEDEN Telephone: +46 10-516 50 00 E-mail: info@ri.se, Internet: www.ri.se	Fire Protection RISE Report 2026:102 ISBN: 978-91-90193-35-8

© RISE Research Institutes of Sweden